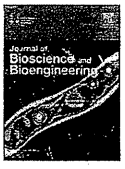

Journal of Bioscience and Bioengineering
VOL. xx No. xx, 1–5, 2014

www.elsevier.com/locate/jbiosc

An *in vitro* liver model consisting of endothelial vascular networks surrounded by human hepatoma cell lines allows for improved hepatitis B virus replication

Sungho Ahn,[1] Miho Tamai,[1] Kenji Nakashima,[2] Masahiko Ito,[2] Tetsuro Suzuki,[2] and Yoh-ichi Tagawa[1,*]

Graduate School of Bioscience and Biotechnology, Tokyo Institute of Technology, 4259 B51, Nagatsuta-cho, Midori-ku, Yokohama, Kanagawa 226-8501, Japan[1] *and Department of Infectious Diseases, Hamamatsu University School of Medicine, 1-20-1 Handayama, Higashi-ku, Hamamatsu, Shizuoka 431-3192, Japan*[2]

Received 2 December 2013; accepted 16 December 2013
Available online xxx

The life cycle of viruses, from infection to budding, is dependent upon the physiological activity of the host cells, such as expression of cell surface proteins, activities of organelles and transcription factors and so on. Human hepatitis viruses exploit multiple hepatocyte pathways during their life cycle; however, primary hepatocytes dramatically lose function and die when cultured as a monolayer *in vitro*. We previously reported the development of an *in vitro* liver model, IVL, consisting of endothelial networks and mouse primary hepatocytes. Hepatocytes cultured using the IVL achieved higher hepatic gene expression and drug sensitivity. In this study, human IVLs were constructed by using the human hepatoma cell lines, Hep G2 and HuH-7, and human umbilical vein endothelial cell networks on Engelbreth-Holm-Swarm gels. In order that these human IVLs could serve as *in vitro* models of human viral hepatitis, these human hepatoma cell lines were stably transfected with the hepatitis B virus (HBV) genome. The levels of HBV markers observed in the supernatant of the IVL cultures were significantly increased as compared to those obtained in transfected monocultures. Furthermore, the hepatocytes in the human IVL cultures became polarized, leading to efficient HBV replication and release *in vitro*. This finding suggests that the IVL culture system could be an effective model for HBV replication.

[**Key words:** Liver; Hepatitis B virus; Hepatic tissue; Polarity; Hepatocyte; Endothelial cell; Tissue engineering]

The life cycle of viruses, from infection to budding, is dependent upon the physiological activity of the host cells. To establish an *in vitro* system that closely mimics the *in vivo* mechanisms underlying viral infection and proliferation, it is important to maintain the host cellular system in a native state, including achieving the appropriate expression of cell surface molecules, and maintaining cell-specific enzyme activities. In liver cells, many of these features depend on signals derived from cell polarity (1). *In vivo*, hepatocytes inhabit a space with cell polarities defined by a variety of neighboring cells and substrates, including adjacent hepatocytes, the extracellular matrix within the space of Disse, and the bile canaliculi. The signals derived from these diverse contacts might contribute to multiple hepatic functions and affect drug pharmacokinetics. Primary hepatocytes prepared from human or animal liver do not proliferate *in vitro* and lose most hepatic functions, e.g., urea production and drug metabolism, during time in culture (2). Several studies attempted to recapitulate hepatic cell polarity *in vitro* by using hepatocyte spheroid culture systems (3–5), or simple co-cultures of hepatocytes and hepatic non-parenchymal cells (6–8). However, as they did not incorporate the liver sinusoidal structure in their design, those culture systems encountered only limited success. Recently, we reported that a reconstructed hepatic tissue structure consisting of a co-culture of mouse primary hepatocytes and human umbilical vein endothelial cells (HUVECs) on Engelbreth-Holm-Swarm (EHS) gel achieved high *in vitro* hepatic gene expression and drug sensitivity (2). We call this hepatic tissue culture system, containing both hepatic cells and endothelial cell networks, an *in vitro* liver model, IVL; our results suggest that it could be a useful model for the *in vitro* study of liver metabolism and disease. The ability to mimic hepatocyte function *in vitro* is important not only for toxicology and pharmacokinetic studies, but also for the development of an artificial liver system, and to establish *in vitro* disease models of human viral hepatitis.

Hepatitis B virus (HBV) is one of the world's most widespread pathogens; it causes both acute and chronic infections, and is associated with severe liver diseases. It is estimated that more than 2 billion people have been infected and about 600,000 people die annually due to the consequences of acute or chronic HBV hepatitis, cirrhosis, and hepatocellular carcinoma (9). Despite these pressing numbers, progress in HBV research has been hampered by the lack of sufficient *in vitro* models of infection and proliferation. Recently, only human and tupaia primary hepatocytes, and a few cell lines, e.g., the human hepatic progenitor cell line, HepaRG, or the immortalized primary hepatocytes, HuS-E/2, have been reported to be susceptible to HBV infection (10–13). HBV studies using the primary hepatocytes or differentiated HepaRG have been restricted because the cells cannot proliferate and survive for long periods *in vitro*. Furthermore, those systems are very costly, limiting their use in vaccine or drug screens. Although other hepatoma cell lines are not susceptible to HBV infection, both Hep G2 cells and HuH-7 cells can support the proliferation of HBV when transfected with a

* Corresponding author. Tel.: +81 45 924 5791; fax: +81 45 924 5809.
E-mail address: ytagawa@bio.titech.ac.jp (Y.-i. Tagawa).

1389-1723/$ – see front matter
http://dx.doi.org/10.1016/j.jbiosc.2013.12.016

plasmid containing the HBV genome (14–16), and those cells have been used to study the HBV life cycle (17). However, since Hep G2 and HuH-7 cells do not accurately represent functional hepatocytes, they cannot precisely reflect HBV gene expression and replication as it occurs in the liver, where metabolism-related transcription factors are required to activate HBV transcription (18).

In this study, to achieve high efficiency of HBV propagation *in vitro*, we constructed human IVLs, consisting of endothelial cell networks surrounded by human hepatoma cell lines. The human hepatoma cell lines incorporated into these IVLs were stably transfected with the HBV genome. Accordingly, HBV markers were significantly increased in IVL culture-conditioned media as compared to the levels observed in the conditioned media of hepatocyte monocultures.

MATERIALS AND METHODS

Cell lines and culture conditions HUVECs (Cambrex BioScience, Walkersville, MD, USA) were cultured in EGM-2 (Lonza Japan Ltd., Tokyo, Japan) on gelatin-coated plates. Mouse adult primary hepatocytes were isolated from male C57BL/6J mice by *in situ* collagenase perfusion and maintained in DMEM containing 10% FBS, 100 U/ml penicillin, and 100 μg/ml streptomycin (19). The human hepatoma cell lines—Hep G2 and its clone Hep G2.2.15, stably transfected with the HBV genome of genotype D-containing plasmid vector (14), and HuH-7, a well-differentiated hepatocellular carcinoma cell line—were cultured in DMEM containing 10% FBS, 100 U/ml penicillin, and 100 μg/ml streptomycin. HuH-7 cells were co-transfected with pUC19 vector carrying 1.24-fold the HBV genome of genotype A (20) and pSV2Neo by using Fugene 6 transfection reagent (Roche Applied Science, Mannheim, Germany), followed by culturing under the medium in the presence of 0.6 mg/ml G418 for 3 weeks. G418-resistant colonies were picked up, and hepatitis B surface antigen (HBsAg) level in conditioned medium of each clone was determined. HuH-HB-Ae, clones which stably replicating HBV genome and expressing viral antigens at high levels were established. To construct an IVL culture system, endothelial cells were seeded on Engelbreth-Holm-Swarm (EHS) gel (BD Biosciences, Bedford, MA, USA). After endothelial cells were attached to the gel, hepatic cells were seeded and cultured for 1 day to adhere. All cells were cultured under an atmosphere of 5% CO_2 at 37°C.

The experiments were conducted according to institutional ethical guidelines for animal experiments and safety guidelines for recombinant DNA experiments.

RNA extraction and reverse transcription-polymerase chain reaction analysis Total RNA was isolated by the acid guanidinium thiocyanate-phenol-chloroform method (21) or by using TRI Reagent (Sigma–Aldrich, St. Louis, MO, USA), and reverse transcription was performed. PCR was performed using Ex *Taq* DNA polymerase (Takara, Tokyo, Japan), and for the quantitative analysis of expression of HBV pregenomic (pg) RNA-expression, real time PCR was conducted using Thunderbird SYBR qPCR Mix (Toyobo, Osaka, Japan) and the primers listed in Supplementary Table S1.

Bile canaliculi functionality Mouse primary hepatocytes, Hep G2, or HuH-7 cells were seeded on HUVEC networks to form IVL structures and were cultured for 24 h. IVLs were washed 3 times with PBS and incubated for 10 min in DMEM containing 2 μg/ml of 5-(and-6)-carboxy-2′,7′-dichlorofluorescein diacetate (CDF-DA). After incubation, IVLs were washed 3 times with PBS and images were acquired with a fluorescence microscope (Leica Microsystems, Wetzlar, Germany).

Quantitation of HBV DNA from cell culture conditioned medium Cell culture conditioned media were collected every day and pooled for 2 days. Glycogen (2 μg) was added to 300 μl of conditioned medium, the solution was added to 1 ml of TNE buffer (10 mM Tris-HCl pH 8.0, 100 mM NaCl, 1 mM EDTA) containing polyethylene glycol, and samples were incubated for 1 h on ice. After centrifugation at 11,500 ×*g* for 15 min at 4°C, the pellets were dissolved in 90 μl of DNase buffer (40 mM Tris-HCl pH 7.5, 8 mM $MgCl_2$ and 5 mM DTT) containing 50 U of DNase I (Takara) and 0.5 μg of RNase A (Roche Applied Science) and further incubated at 37°C for 1 h to eliminate unpackaged nucleic acids. Next, 10 μl of 20 mg/ml Proteinase K solution (Wako, Osaka, Japan) with 300 μl of Proteinase K buffer (10 mM Tris-Cl pH 8.0, 0.5% SDS and 5 mM EDTA) were added to the solution and incubated at 56°C for 2 h to digest viral particles. DNA was extracted using phenol-chloroform-isoamyl alcohol, and precipitated with ethanol. Pellets were dissolved in 1/10 TE buffer, and subjected to real time PCR.

RESULTS

Construction of an *in vitro* liver model consisting of endothelial cell vascular networks and human hepatoma cell lines HUVECs were seeded at 4.2×10^4 cells/cm^2 on EHS gel and formed structural networks within 12 h (Fig. 1A). Mouse primary hepatocytes, the human hepatocellular carcinoma cell line, Hep G2, or the well-differentiated human hepatoma cell line, HuH-7, were seeded at 1.2×10^5 cells/cm^2 on the HUVEC networks. All of the tested hepatocytes and hepatoma cells migrated toward the HUVEC networks as shown in Fig. 1B–D. The *in vitro* liver models consisting of HUVEC networks and either the Hep G2 or HuH-7 cells on EHS gel were termed IVL$^{\text{Hep G2/HuH-7}}$. The expression of liver-specific genes, e.g., *ALB*, *TAT*, *C/EBPα*, and *HNF4α* was much higher in IVL$^{\text{Hep G2/HuH-7}}$ as compared to levels observed in co-cultures on gelatin (Fig. 1E). Interestingly, the expression of some transporter genes, e.g., *OATP8*, *OCT1*, and *MRP2*, was also enhanced in or specific to IVL$^{\text{Hep G2}}$ as compared to the other culture conditions. *MRP2* expression was also strongly detected in IVL$^{\text{HuH-7}}$. These transporters specifically localize to sinusoidal or bile canalicular membranes of

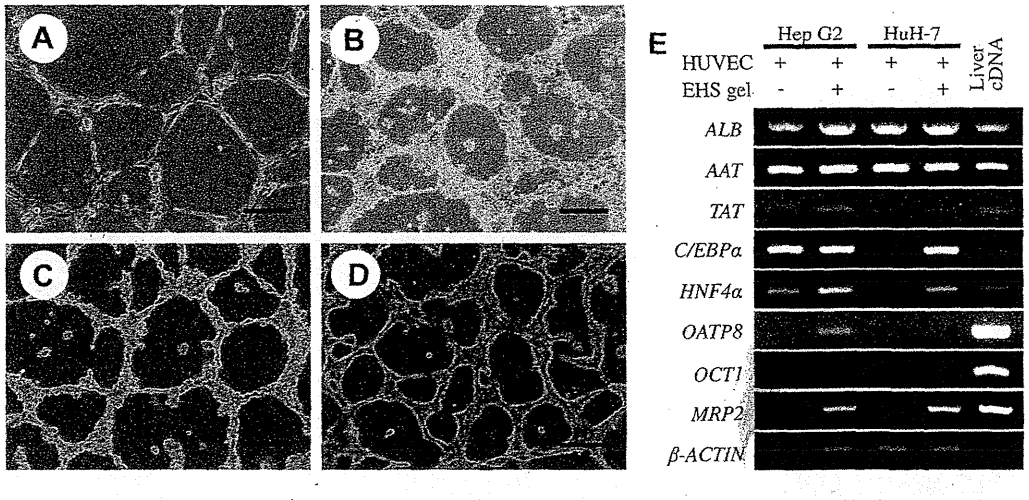

FIG. 1. The morphology of co-cultures containing HUVECs and either mouse primary hepatocytes or human hepatoma cell lines on EHS gels. A single culture of HUVECs on EHS gel (A), a co-culture of HUVECs and murine primary hepatocyte (IVL$^{\text{PrH}}$) on EHS gel (B), a co-culture of HUVECs and human Hep G2 cells (IVL$^{\text{Hep G2}}$) on EHS gel (C), and a co-culture of HUVECs and human HuH-7 cells (IVL$^{\text{HuH-7}}$) on EHS gel (D) at 24 h. Scale bars: 200 μm. (E) RT-PCR analysis of gene expression in IVL$^{\text{Hep G2/HuH-7}}$ cultures. The expression of each gene was compared among co-cultures plated either on gelatin or on EHS gel. Genes examined: *ALB*, albumin; *AAT*, alpha 1-antitrypsin; TAT, tyrosine aminotransferase; C/EBPα, CCAAT/enhancer binding protein α; HNF4α, hepatocyte nuclear factor 4α; OATP8, organic anion transporting polypeptide 8; OCT1, organic cation transporter 1; MRP2, multidrug resistance-associated protein 2.

Please cite this article in press as: Ahn, S., et al., An *in vitro* liver model consisting of endothelial vascular networks surrounded by human hepatoma cell lines allows for improved hepatitis B virus replication, J. Biosci. Bioeng., (2014), http://dx.doi.org/10.1016/j.jbiosc.2013.12.016

hepatocyte. In order to investigate the combinations of transporters and cellular enzymes, CDF-DA was added at a final concentration of 2 μg/ml to the culture medium. An accumulation of hydrolyzed CDF, detected as green fluorescence, was observed in IVL of mouse primary hepatocytes and $IVL^{Hep\ G2/HuH-7}$ (Fig. 2A–C). By contrast, CDF accumulation was not observed in monocultures of mouse primary hepatocytes, Hep G2, or HuH-7 cells on gelatin, although a weak signal was detected in the cytoplasm of all the cells (Fig. 2D–F). These results suggested that hepatic cells cultured in the context of IVL can maintain hepatic functions at a higher level as compared to hepatocytes cultured on gelatin due to the induction of cell polarity.

The proliferation of HBV in $IVL^{Hep\ G2.2.15}$ and $IVL^{HuH-HB-Ae}$ Because hepatocyte polarity induced by the IVL could lead to an upregulation of hepatic functions, the replication and expression of HBV genes were investigated in IVL cultures. Hep G2.2.15 cells, which can achieve continuous HBV proliferation and release of viral particles into their culture medium, were seeded at 1.2×10^5 cells/cm^2 on HUVEC networks. The Hep G2.2.15 cells migrated toward the networks and IVL-specific structures were observed (Fig. 3A). Meanwhile, Hep G2.2.15 cells formed aggregates in monocultures on EHS gel (Fig. 3B), and no specific structures were seen in Hep G2.2.15 cells cultured on type I collagen, either with (Fig. 3C) or without HUVECs (Fig. 3D). To investigate the intracellular HBV proliferation of $IVL^{Hep\ G2.2.15}$, total RNA was extracted from the cell pellet on day 7 of the culture, and semi-quantitative RT-PCR analysis of HBV pregenomic RNA (pgRNA), which is a replication intermediate of HBV, was performed. Co-cultures of Hep G2.2.15 cells and HUVECs yielded higher levels of HBV pgRNA than did monocultures on either EHS gel or type I collagen; no significant differences were observed between cultures on the two materials (Fig. 3E). Moreover, HBV particle-associated DNA levels in the culture supernatants, indicating the amount of released HBV particles, were significantly higher after 3–5 days in $IVL^{Hep\ G2.2.15}$ cultures as compared to those observed in co-cultures on type I collagen (Fig. 3F).

To investigate in other hepatoma cell line and other genotype of HBV, HuH-7 cells were transfected with an HBV genome of genotype A-containing plasmid. Clones were derived and a cell line, HuH-HB-Ae, constitutively expressing the HBV gene was established and used in our IVL system ($IVL^{HuH-HB-Ae}$). As was the case for mouse primary hepatocytes and Hep G2.2.15 cells, HuH-HB-Ae cells formed an IVL structure when seeded at 1.2×10^5 cells/cm^2 on HUVEC networks (Fig. 4A), but not when cultured in the absence of either HUVEC cells or EHS gel (Fig. 4B–D). As determined by enzyme immunoassay (EIA), cell culture supernatants from $IVL^{HuH-HB-Ae}$ cultures exhibited significantly higher levels of HBsAg as compared to the other culture conditions (Fig. 4E). Together, these results indicate that the replication of HBV genome and/or release efficiency of HBV viral particles was improved when liver-specific tissue structures were formed.

DISCUSSION

Hep G2 and HuH-7 cells have been used as model systems for HBV replication, and as such, have been transfected *in vitro* with HBV DNA (14,22,23). However, these models are not sufficiently robust; for example, they suffer from low efficiency of viral gene expression, and inefficient assembly and release of infectious particles. Recently, some cell surface factors, localized on polarized hepatocytes in the liver, have been reported to be necessary for infection by HBV (24,25) and HCV (23,26). In addition to cell polarization, it may be necessary to mimic other aspects of mature hepatocyte physiology in order to develop an *in vitro* model of the HBV life cycle in human liver. In this study, we generated IVLs consisting of endothelial cell networks and either mouse primary hepatocytes or human Hep G2 or HuH-7 cells (2). These IVLs exhibited hepatocyte-specific gene expression (Fig. 1E), strong hepatic function, and cell polarity (Fig. 2A–C). Because histological examination indicated that the HUVEC networks formed tube structures (data not shown) that were surrounded by hepatocytes in the IVL, the IVL micro-architecture resembled liver sinusoids (2,27).

CDF-DA is incorporated into hepatocytes via the transporters OATP2 or organic anion transporting polypeptide 8 (OATP8), and is hydrolyzed to its fluorescent form (CDF) by cytoplasmic esterases. Finally, CDF is released into bile canaliculi via the transporter multidrug resistanceassociated protein 2 (MRP2) (28). Cell polarity can be induced in spheroid cultures of Hep G2 (23), although Hep G2 in two-dimensional co-cultures did not express OATPs, and thus did not incorporate CDF-DA (Fig. 1E), or release fluorescent CDF (Fig. 2E). By contrast, the expression of the transporter genes, *OATP8*, *OCT1*, and *MRP2*, was strongly detected in $IVL^{Hep\ G2}$ (Fig. 1E), and the accumulation of fluorescent CDF was observed in all of the

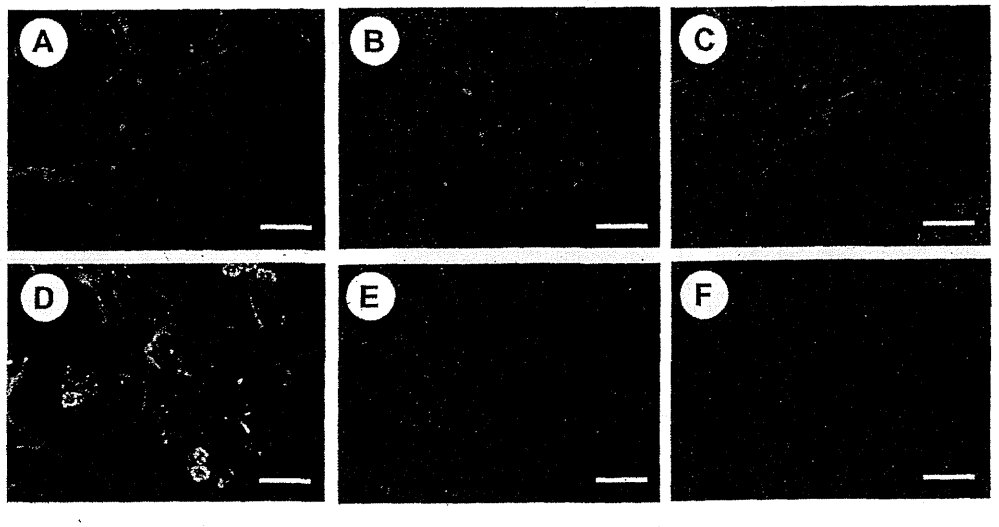

FIG. 2. Incorporation, hydrolysis, and excretion of CDF-DA in the IVLs. (A–C) IVLs containing either mouse primary hepatocytes (A), Hep G2 cells (B), or HuH-7 cells (C). (D–F) Simple two-dimensional cultures on gelatin of mouse primary hepatocytes (D), Hep G2 cells (E), or HuH-7 cells (F). Green fluorescence indicates the accumulation of hydrolyzed CDF. Scale bars: 100 μm (For interpretation of the references to color in this figure legend, the reader is referred to the web version of this article.).

Please cite this article in press as: Ahn, S., et al., An *in vitro* liver model consisting of endothelial vascular networks surrounded by human hepatoma cell lines allows for improved hepatitis B virus replication, J. Biosci. Bioeng., (2014), http://dx.doi.org/10.1016/j.jbiosc.2013.12.016

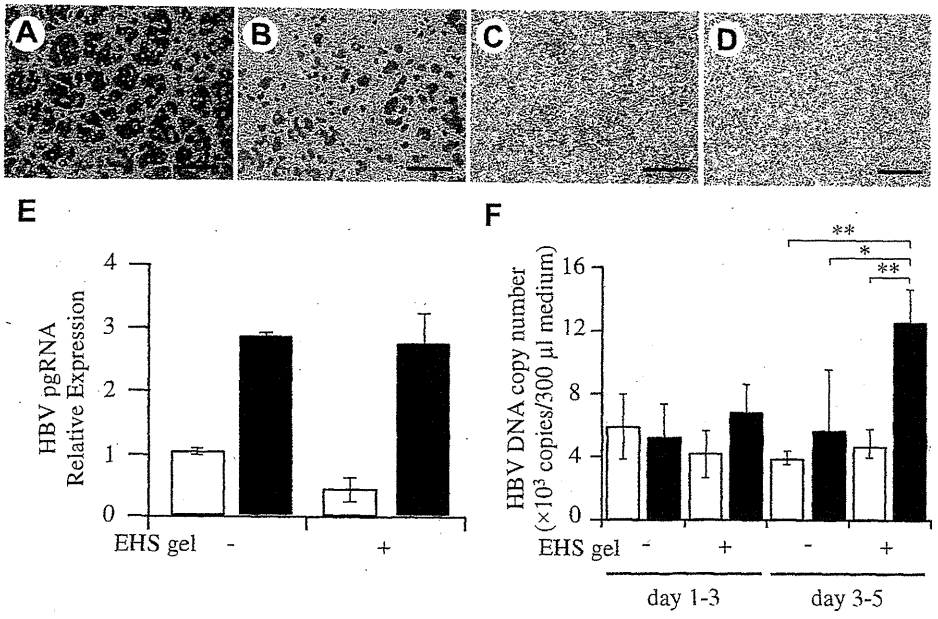

FIG. 3. HBV replication in IVL$^{Hep\ G2.2.15}$. (A, B) The morphology of Hep G2.2.15 cells cultured with (A) or without (B) HUVECs on EHS gel. (C, D) The morphology of Hep G2.2.15 cells cultured with (C) or without (D) HUVECs on collagen type I. Scale bars: 500 µm. (E) The intracellular expression of HBV pgRNA on day 7. (F) Quantitation of HBV DNA in the cell culture medium. Open bars, HUVEC (−); closed bars, HUVEC (+). Data mean ± S.E., $^{*}p < 0.05$, $^{**}p < 0.005$.

IVL iterations (Fig. 2A–C). Conversely, neither the transporter gene expression nor the CDF accumulation was noted in the control co-cultures plated on gelatin (Fig. 2D–F). In IVL^{HuH-7}, *MRP2* expression was strongly detected, but *OATP8* expression was not found (Fig. 1E). The expression of additional transporters may account for the incorporation of CDF-DA into the hepatocytes in IVL^{HuH-7}, which were able to accumulate fluorescent CDF (Fig. 2C).

HBV gene expression is regulated at the transcriptional level via enhancers I and II, and by four promoters, i.e., S, C, P, and X. The enhancer II region, in particular, is reported to be a hepatocyte-specific regulatory system, due to the prevalence of binding sites for hepatocyte-enriched transcription factors and nuclear receptors, e.g., CCAAT/enhancer binding protein (C/EBP), forkhead Box O1, the hepatocyte nuclear factor (HNF) families, farnesoid X receptor, and peroxisome proliferator-activated receptors, which are recruited to the enhancer II region and activate viral gene expression (18). In this study, the expression of *C/EBPα* and *HNF4α* was significantly elevated in IVL$^{Hep\ G2/HuH-7}$ as compared to similar co-cultures plated on gelatin (Fig. 1E). Those transcription factors control hepatocyte-specific gene expression and hepatocyte metabolism. As shown in Fig. 1E, the expression of *ALB* and *TAT* was up-regulated in IVL$^{Hep\ G2/HuH-7}$, indicating that the expression of hepatocyte-specific transcription factors was enriched through co-culture with endothelial cell networks on EHS gel, leading to an enhancement of HBV replication in this culture system.

Particle-associated HBV DNA levels were higher in IVL$^{Hep\ G2.2.15}$ (Fig. 3F), and released HBsAg levels were significantly higher in IVL$^{HuH-HB-Ae}$ (Fig. 4E), despite the lack of significant differences in the intracellular expression of pgRNA (Fig. 3E). These results indicated that viral particle release may depend on cell polarity; further investigation is warranted.

In conclusion, we demonstrated a novel hepatic tissue culture system, IVL, which forms specific hepatic tissue structures consisting of hepatocytes surrounding endothelial cell networks. Transfection of these cultures with HBV DNA led to an increased release of HBV particles and HBsAg into the conditioned medium as compared to that observed in non-IVL transfected cultures. The human hepatoma cell lines, Hep G2 and HuH-7 and their subclones, were used in this study, but this IVL model could also be implemented with a combination of human ES/iPS cell-derived

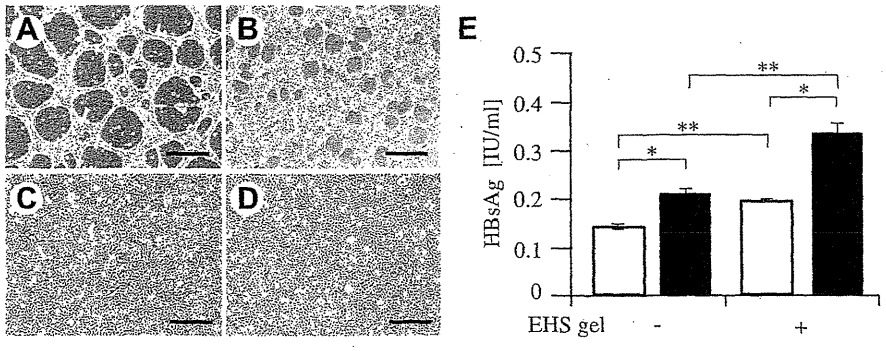

FIG. 4. HBV replication in IVL$^{HuH-HB-Ae}$. (A, B) The morphology of HuH-HB-Ae cells cultured with (A) or without (B) HUVECs on EHS gel. (C, D) The morphology of HuH-HB-Ae cells cultured with (C) or without (D) HUVECs ~~collagen type I~~. Scale bars: 500 µm. (E) Quantitation of released HBsAg on days 1–3. Open bars, HUVEC (−); closed bars, HUVEC (+). Data mean ± S.E., $^{*}p < 0.05$, $^{**}p < 0.005$.

Please cite this article in press as: Ahn, S., et al., An *in vitro* liver model consisting of endothelial vascular networks surrounded by human hepatoma cell lines allows for improved hepatitis B virus replication, J. Biosci. Bioeng., (2014), http://dx.doi.org/10.1016/j.jbiosc.2013.12.016

hepatocytes. An IVL culture system comprising human ES/iPS cell-derived hepatocytes might be an efficient tool to provide new insight into the HBV life cycle, which requires close fidelity to the *in vivo* human liver tissue structure for its study.

Supplementary data related to this article can be found at http://dx.doi.org/10.1016/j.jbiosc.2013.12.016.

ACKNOWLEDGMENTS

This study was supported by a Health and Labor Sciences Research Grant from the Ministry of Health, Precursory Research for Embryonic Science and Technology (PRESTO) from the Japan Science and Technology Agency (JST), by a Scientific Research (A) (no. 25242040) award from the Japan Society for the Promotion of Science (JSPS), and by a Grant-in-Aid for Scientific Research on Innovative Areas (no. 231190003) from the Ministry of Education, Culture, Sports, Science and Technology of Japan (MEXT). The plasmid of HBV genome of genotype A was kindly provided by Dr. Masashi Mizokami from ~~Nagoya City University~~.

References

1. **Teyer, A. and Müsch, A.:** Hepatocyte polarity. Compr. Physiol., **3**, 243–287 (2013).
2. **Toyoda, Y., Tamai, M., Kashikura, K., Kobayashi, S., Fujiyama, Y., Soga, T., and Tagawa, Y.:** Acetaminophen-induced hepatotoxicity in a liver tissue model consisting of primary hepatocytes assembling around an endothelial cell network, Drug Metab. Dispos., **40**, 169–177 (2011).
3. **Landry, J., Bernier, D., Ouellet, C., Goyette, R., and Marceau, N.:** Spheroidal aggregate culture of rat liver cells: histotypic reorganization, biomatrix deposition, and maintenance of functional activities, J. Cell Biol., **101**, 914–923 (1985).
4. **Brophy, C. M., Luebke-Wheeler, J. L., Amiot, B. P., Khan, H., Remmel, R. P., Rinaldo, P., and Nyberg, S. L.:** Rat hepatocyte spheroids formed by rocked technique maintain differentiated hepatocyte gene expression and function, Hepatology, **49**, 578–586 (2009).
5. **Glicklis, R., Merchuk, J. C., and Cohen, S.:** Modeling mass transfer in hepatocyte spheroids via cell viability, spheroid size, and hepatocellular functions, Biotechnol. Bioeng., **86**, 672–680 (2004).
6. **Bhatia, S. N., Balis, U. J., Yarmush, M. L., and Toner, M.:** Effect of cell-cell interactions in preservation of cellular phenotype: cocultivation of hepatocytes and nonparenchymal cells, FASEB J., **13**, 1883–1900 (1999).
7. **Kidambi, S., Yarmush, R. S., Novik, E., Chao, P., Yarmush, M. L., and Nahmias, Y.:** Oxygen-mediated enhancement of primary hepatocyte metabolism, functional polarization, gene expression, and drug clearance, Proc. Natl. Acad. Sci. USA, **106**, 15714–15719 (2009).
8. **Krause, P., Saghatolislam, F., Koenig, S., Unthan-Fechner, K., and Probst, I.:** Maintaining hepatocyte differentiation in vitro through co-culture with hepatic stellate cells, In Vitro Cell. Dev. Biol. Anim., **45**, 205–212 (2009).
9. **World Health Organization:** Prevention and control of viral hepatitis infection: a frame work for global action, pp. 1–28, World Health Organization, Geneva (2012).
10. **Gripon, P., Diot, C., Thézé, N., Fourel, I., Loreal, O., Brechot, C., and Guguen-Guillouzo, C.:** Hepatitis B virus infection of adult human hepatocytes cultured in the presence of dimethyl sulfoxide, J. Virol., **62**, 4136–4143 (1988).
11. **Ochiya, T., Tsurimoto, T., Ueda, K., Okubo, K., Shiozawa, M., and Matsubara, K.:** An in vitro system for infection with hepatitis B virus that uses primary human fetal hepatocytes, Proc. Natl. Acad. Sci. USA, **86**, 1875–1879 (1989).
12. **Gripon, P., Rumin, S., Urban, S., Le Seyec, J., Glaise, D., Cannie, I., Guyomard, C., Lucas, J., Trepo, C., and Guguen-Guillouzo, C.:** Infection of a human hepatoma cell line by hepatitis B virus, Proc. Natl. Acad. Sci. USA, **99**, 15655–15660 (2002).
13. **Huang, H. C., Chen, C. C., Chang, W. C., Tao, M. H., and Huang, C.:** Entry of hepatitis B virus into immortalized human primary hepatocytes by clathrin-dependent endocytosis, J. Virol., **86**, 9443–9453 (2012).
14. **Sells, M. A., Chen, M. L., and Acs, G.:** Production of hepatitis B virus particles in Hep G2 cells transfected with cloned hepatitis B virus DNA, Proc. Natl. Acad. Sci. USA, **84**, 1005–1009 (1987).
15. **Ladner, S. K., Otto, M. J., Barker, C. S., Zaifert, K., Wang, G. H., Guo, J. T., Seeger, C., and King, R. W.:** Inducible expression of human hepatitis B virus (HBV) in stably transfected hepatoblastoma cells: a novel system for screening potential inhibitors of HBV replication, Antimicrob. Agents Chemother., **41**, 1715–1720 (1997).
16. **Gouskos, T., Wightman, F., Lewin, S. R., and Torresi, J.:** Highly reproducible transient transfections for the study of hepatitis B virus replication based on an internal GFP reporter system, J. Virol. Methods, **121**, 65–72 (2004).
17. **Liang, T. J.:** Hepatitis B: the virus and disease, Hepatology, **49**, S13–S21 (2009).
18. **Bar-Yishay, I., Shaul, Y., and Shlomai, A.:** Hepatocyte metabolic signalling pathways and regulation of hepatitis B virus expression, Liver Int., **31**, 282–290 (2011).
19. **Tamai, M., Adachi, E., and Tagawa, Y.:** Characterization of a liver organoid tissue composed of hepatocytes and fibroblasts in dense collagen fibrils, Tissue Eng. Part A, **19**, 2527–2535 (2013).
20. **Sugiyama, M., Tanaka, Y., Kato, T., Orito, E., Ito, K., Acharya, S. K., Gish, R. G., Kramvis, A., Shimada, T., Izumi, N., and other 3 authors:** Influence of hepatitis B virus genotypes on the intra- and extracellular expression of viral DNA and antigens, Hepatology, **44**, 915–924 (2006).
21. **Tamai, M., Yamashita, A., and Tagawa, Y.:** Mitochondrial development of the in vitro hepatic organogenesis model with simultaneous cardiac mesoderm differentiation from murine induced pluripotent stem cells, J. Biosci. Bioeng., **112**, 495–500 (2011).
22. **Chang, C. M., Jeng, K. S., Hu, C. P., Lo, S. J., Su, T. S., Ting, L. P., Chou, C. K., Han, S. H., Pfaff, E., and Salfeld, J.:** Production of hepatitis B virus in vitro by transient expression of cloned HBV DNA in a hepatoma cell line, EMBO J., **6**, 675–680 (1987).
23. **Mee, C. J., Harris, H. J., Farquhar, M. J., Wilson, G., Reynolds, G., Davis, C., van Ijzendoorn, S. C. D., Balfe, P., and McKeating, J. A.:** Polarization restricts hepatitis C virus entry into HepG2 hepatoma cells, J. Virol., **83**, 6211–6221 (2009).
24. **Schulze, A., Mills, K., Weiss, T. S., and Urban, S.:** Hepatocyte polarization is essential for the productive entry of the hepatitis B virus, Hepatology, **55**, 373–383 (2011).
25. **Yan, H., Zhong, G., Xu, G., He, W., Jing, Z., Gao, Z., Huang, Y., Qi, Y., Peng, B., Wang, H., and other 10 authors:** Sodium taurocholate cotransporting polypeptide is a functional receptor for human hepatitis B and D virus, eLife, **1**, e00049 (2012).
26. **Molina-Jimenez, F., Benedicto, I., Thi, V. L. D., Gondar, V., Lavillette, D., Marin, J. J., Briz, O., Moreno-Otero, R., Aldabe, R., Baumert, T. F., and other 3 authors:** Matrigel-embedded 3D culture of Huh-7 cells as a hepatocyte-like polarized system to study hepatitis C virus cycle, Virology, **425**, 31–39 (2012).
27. **Nahmias, Y., Schwartz, R. E., Hu, W.-S., Verfaillie, C. M., and Odde, D. J.:** Endothelium-mediated hepatocyte recruitment in the establishment of liver-like tissue in vitro, Tissue Eng., **12**, 1627–1638 (2006).
28. **Zamek-Gliszczynski, M. J.:** Pharmacokinetics of 5 (and 6)-carboxy-2′,7′-dichlorofluorescein and its diacetate promoiety in the liver, J. Pharmacol. Exp. Ther., **304**, 801–809 (2003).

Please cite this article in press as: Ahn, S., et al., An *in vitro* liver model consisting of endothelial vascular networks surrounded by human hepatoma cell lines allows for improved hepatitis B virus replication, J. Biosci. Bioeng., (2014), http://dx.doi.org/10.1016/j.jbiosc.2013.12.016

Journal of Bioscience and Bioengineering
VOL. 117 No. 3, 358–365, 2014

www.elsevier.com/locate/jbiosc

Innate immunity in an *in vitro* murine blastocyst model using embryonic and trophoblast stem cells

Hiroaki Aikawa,[1] Miho Tamai,[1] Keisuke Mitamura,[1] Fakhria Itmainati,[1] Glen N. Barber,[2] and Yoh-ichi Tagawa[1,*]

Department of Biomolecular Engineering, Graduate School of Bioscience and Biotechnology, Tokyo Institute of Technology, 4259 B51, Nagatsuta-cho, Midori-ku, Yokohama-shi, Kanagawa 226-8501, Japan[1] and Department of Medicine and Sylvester Comprehensive Cancer Center, University of Miami Miller School of Medicine, Rm 511 Papanicolaou Building, 1550 NW 10th Ave, Miami, FL 33136, USA[2]

Received 21 June 2013; accepted 2 September 2013
Available online 7 October 2013

The immune system has two broad components—innate and adaptive immunity. Adaptive immunity becomes established only after the onset of hematopoiesis, whereas the innate immune system may be actively protecting organisms from microbial invasion much earlier in development. Here, we address the question of whether the innate immune system functions in the early-stage embryo, i.e., the blastocyst. The innate immune system was studied by using *in vitro* blastocyst models, e.g., embryonic stem (ES) and trophoblast stem (TS) cell cultures. The expression of Toll-like receptors (TLR)-2, -3, and -5 could be detected in both ES and TS cells. The expression of interferon (IFN)-β was induced by the addition of polyinosinic:polycytidylic acid [poly(I:C)] in TS cells, but not ES cells, although TLR-3 was expressed at the same level in both cell types. In turn, ES cells responded to IFN-β exposure by expressing IFN-induced anti-viral genes, e.g., RNA-dependent protein kinase and 2′, 5′-oligoadenylate synthetase (OAS). Neither a reduction in ES cell proliferation nor cell death in these cultures was observed after IFN-β stimulation. Furthermore, OAS1a expression was induced in ES/TS co-cultures after poly(I:C) stimulation, but was not induced when either cell type was cultured alone. In conclusion, TS cells react to poly(I:C) stimulation by producing IFN-β, which induces IFN-inducible genes in ES cells. This observation suggests that the trophectoderm, the outer layer of the blastocyst, may respond to viral infection, and then induce anti-viral gene expression via IFN-β signaling to the blastocyst inner cell mass.

[**Key words:** Innate immunity; Blastocyst; Trophoblast stem cell; Embryonic stem cell; Toll-like receptors; Type-I interferon]

The immune system largely consists of two broad components—innate and adaptive immunity (1). In turn, adaptive immunity comprises humoral immunity, largely governed by B cells that produce high-affinity antibodies, and cellular immunity, largely governed by T cells that recognize processed peptide antigens presented by antigen presenting cells in the context of the major histocompatibility complex proteins. During development, the adaptive immune system is established after the initiation of hematopoiesis, which gives rise to B and T cells, among others (2). By contrast, innate immunity is an evolutionarily conserved system that provides a first line of protection against invading microbial pathogens and is activated by Type-I and III interferons (IFNs) (3,4). Most types of mammalian cells can produce IFNs upon viral infection by sensing cytoplasmic non-self DNA or RNA, or by recognizing pathogenic molecular signatures via 'pattern recognition receptors', e.g., Toll-like receptors (TLRs), Sting, and RIG-I–like receptors. TLRs are evolutionarily conserved membrane proteins that are critical for the activation of mammalian innate immunity (5). TLR signaling leads to the production of IFNs, which, in turn, induce the expression of anti-viral proteins, such as RNA-dependent protein kinase (PKR) and 2′, 5′-oligoadenylate synthetase (OAS) (3).

The innate immune system is functional in insects (6–8), which have no lymphocytes (T or B cells). Because the mammalian embryo, prior to the onset of hematopoiesis, has no adaptive immune system, another defense system is necessary. The innate immune system is functional in mice by embryonic day 12–13 post-coitum (E12–13) as demonstrated by the fact that mouse embryonic fibroblasts (MEFs), which are generally prepared from E12–13 embryos, have a strong innate immune response, i.e., IFN-β expression is strongly induced after TLR stimulation (9–11). The innate immune system likely plays a major role in protecting against microbial invasion before hematopoiesis is established. Hematopoiesis begins in the yolk sac at E7.5 (12). The purpose of this study was to investigate whether the innate immune system has been established in the early-stage embryo, i.e., in the blastocyst before implantation into the uterus. The blastocyst consists of the inner cell mass (ICM), which gives rise to the body of the organism, including the germ cells, and the trophectoderm, which gives rise to the placenta. The blastocyst is surrounded by the zona pellucida (ZP). Early-stage embryos, from the non-fertilized egg to the pre-hatched blastocyst, are surrounded by the zona pellucida,

* Corresponding author. Tel.: +81 45 924 5791; fax: +81 45 924 5809.
E-mail address: ytagawa@bio.titech.ac.jp (Y. Tagawa).

1389-1723/$ – see front matter
http://dx.doi.org/10.1016/j.jbiosc.2013.09.001

which may serve as a barrier from viruses and bacteria that exist in the oviduct and uterus. After the blastocyst hatches from and releases the zona pellucida, the bare blastocyst is exposed to infectious hazards, such as viruses and bacteria in the uterus. Because embryonic stem (ES) cells are derived from the ICM (13), ES cells are thought to be an *in vitro* model of ICM, and their differentiated cells might mimic the developing embryo. The ICM is surrounded in the blastocyst by a trophectoderm layer. Some foreign substances could pass through the ZP and come into contact with the trophectoderm. Because the trophoblast stem (TS) cell line is derived from blastocyst trophectoderm, it might be useful to investigate the behavior of TS cells as an *in vitro* model of the immunological roles of trophectoderm in blastocyst development.

Due to the comparatively easier access to ES cells as compared to TS cells, there are a few reports about the expression of TLRs in ES cells derived from the 129 mouse strain (14–16), but no reports as yet in TS cells. In this study, we began by establishing a mouse TS cell line from the BALB/cA mouse strain, which is of the same origin as the mouse ES cell line, ST1 (17). Then, we investigated the TLR expression patterns and innate immune responses in ES and TS cells, and their co-culture as an *in vitro* blastocyst model, to test whether the blastocyst may have the components for a functioning innate immune system.

MATERIALS AND METHODS

Preparation and culture of early-stage mouse embryos 2.5-day embryos were collected from superovulated BALB/cAJcl female mice (CLEA Japan, Tokyo, Japan) crossed with BALB/cAJcl male mice (CLEA Japan). 2.5-day embryos were cultured for one day in Brinster's BMOC-3 medium (Life Technologies Japan, Tokyo, Japan) to develop into blastocysts. The animal protocol was approved by the Animal Experimentation Committee of the Tokyo Institute of Technology.

Cell culture All cells were cultured at 37°C in a humidified 5% CO_2 atmosphere. The mouse ES cell line, ST1, was originally established from the BALB/c strain (17). ST1 cells were grown on feeder layers of mitomycin C–treated MEFs in order to maintain stem cells in an undifferentiated state, as previously described (18). In this study, to remove MEF cells, ST1 cells were cultured on gelatin-coated plates without the MEF feeder layer in ESGRO Complete PLUS Clonal Grade medium (Chemicon, Temecula, CA, USA). TS cell line, CAT1, was originally established on MEF feeder layer in TS medium supplemented with 25 ng/mL human recombinant FGF4 (R&D Systems, MN, USA) and 1 μg/mL heparin (Sigma–Aldrich Japan, Tokyo, Japan). TS medium is RPMI 1640 medium (Life Technologies Japan) with 20% heat-inactivated fetal bovine serum (FBS; Nichirei Biosciences, Tokyo, Japan), 1 mM sodium pyruvate (Life Technologies Japan), 100 μM 2-mercaptoethanol (Sigma–Aldrich Japan), 2 mM L-glutamine, penicillin and streptomycin (Life Technologies Japan) (19). MEF conditioned medium was collected after three days culture on MEF feeder cells in TS medium. To remove MEF cells for this study, CAT1 cells were cultured on gelatin-coated dishes in 70% MEF conditioned medium/TS medium with FGF4 and heparin. The mouse monocyte–macrophage cell line, RAW264 (RIKEN Cell Bank, Ibaraki, Japan), was cultured in MEM supplemented with 10% FBS and penicillin and streptomycin (Life Technologies Japan). MEF was cultured in DMEM (Life Technologies Japan) with 10% FBS, penicillin and streptomycin (Life Technologies Japan). For co-cultures stimulated by polyinosinic:polycytidylic acid [poly(I:C)], we used GFP-expressing ST1 and DsRed-expressing CAT1.

Establishment of the cell lines carrying DsRed2 or AcGFP expression vector The expression vectors of DsRed2 and AcGFP fluorescence protein genes, pCAGDsRed2-neo and pCAGAcGFP-neo, respectively, were controlled by the CAG promoter (20–23). These expression vectors were introduced in the CAT1 or ST1 cells by the electroporation method as described previously (23). Briefly, 1×10^7 cells/0.9 mL in PBS of the cells was mixed with 25 μg of linearized pCAGDsRed2-neo/Eco RI or pCAGAcGFP-neo/Eco RI, respectively, and were transfected by electroporation method. After electroporation, the cells were seeded onto 100-mm diameter gelatin-coated plastic dishes. The culture medium containing 400 μg/mL or 1 mg/mL G418 was changed at a day after the electroporation. G418-resistant colonies were picked up. The clones were maintained as well as the parental cells were. The expression of those clones was confirmed by the flow cytometer (Beckman Coulter, CA, USA), and then finally each clone with the strongest expression of the DsRed2 or AcGFP gene was established as $CAT1^{Red}$ or $ST1^{Green}$ cell line, respectively.

RT-PCR and real-time PCR Total RNA was isolated using a kit from Kurabo (Tokyo, Japan). After genomic DNA was removed by treatment with DNase I (Promega, Tokyo, Japan), the RNA samples (5 μg) were reverse transcribed using a Superscript II First-Strand Synthesis System Kit (Life Technologies Japan) with an oligo(dT) primer (Life Technologies Japan). PCR was performed using Ex Taq DNA polymerase (Life Technologies Japan) with the primer sets shown in Table 1. For the quantitative analysis of IFN-β, OAS1a, and PKR expression, real-time PCR was carried out using the StepOnePlus Sequence Detection System (Applied Biosystems, Tokyo, Japan). Hypoxanthine-guanine phosphoribosyltransferase (*Hprt*) was used as an internal housekeeping reference gene. Gene expression was quantified using the $\Delta\Delta C_T$ method. Primer sequences are listed in Table 1.

TABLE 1. Primer information for RT-, real-time, and genomic PCR.

primer	Forward Sequence	Reverse Sequence
Toll-like receptor 1	GAGTGTTTGTGAATGCAGTTGG	TAGCTCATTGTGGGACAAATCC
Toll-like receptor 2	TAGGGGCTTCACTTCTCTGC	GAGACTCCTGAGCAGAACAGC
Toll-like receptor 3	ACTGGATGGCCATTTTTACC	AGAGAACAGGTGCGTCAACC
Toll-like receptor 4	TTCTTCTCCTGCCTGACACC	TTCCTGGGGAAAAACTCTGG
Toll-like receptor 5	CCAGACACATCTGTGAGACACC	GCATCTCGATTCAAGACTTCG
Toll-like receptor 6	AAGAAAATGGTACCGTCAGTG CTGG	AAGGCCAGGGCGCAAACAAAGT
Toll-like receptor 7	CCTTCAAGAAAGATGTCCTTGG	GGAGAGATGCTTGGTATGTGG
Toll-like receptor 8	GAGAAACAAACGTTTTACCTTCC	TTTCAAAGACTCAGGCAACC
Toll-like receptor 9	TCTGAGAGACCCTGGTGTGG	AAACGGGGTACAGACTTCAGG
RIG-I	TGCCACAGTCAGAGACAACG	TGCCATCTGAAACACTGAGC
MDA5	GCGGGAATGAGTCAGGTGTAA	GGCTCGGGGGATACTCTTTTT
IPS-1/MAVS	TGCTGTGTTGACGTTCTGG	AAACTCGAGTCACTTGATCAGC
Sting	CCCGAGTCTCGAAATAACTGC	TGAGGAGTCTTGGCTCTTGG
Oct3/4	TTGGAGAAGGTGGAACCAAC	AGATGGTGGTCTGGCTGAAC
Cdx2	GAAACCTGTGCGAGTGGATG	GCAGCCAGCTCACTTTTCCT
IFNAR1	ATGGGACTACATTGCGTCTGC	TTCTTGAGGGTGAACTCTGG
Hprt	GTAATGATCAGTCAACGGGG	AGCTTTACTAGGCAGATGGC
IFN-β (real-time)	CAGGCAACCTTTAAGCATCAG	CTTTGACCTTTCAAATGCAG
PKR (real-time)	GGAAAATCCCGAACAAGGAG	CCCAAAGCAAAGATGTCCAC
OAS1a (real-time)	TGTCCTGGGTCATGTTAATAC	CCGTGAAGCAGGTAGAGA
Hprt (real-time)	TCCTCCTCAGACCGCTTTT	CCTGGTTCATCATCGCTAATC
Sry (genomic)	GCCCTTTTTCCAGGAGGCA	CAGTGGGGATATCAACAGGCT
Hprt (genomic)	TCTCGAAGTGTTGGATACAGGC	AGCTTTACTAGGCAGATGGC

Genomic PCR Genomic DNA was prepared from mouse cells or tissue using a kit from Kurabo. Genomic PCR was performed using Ex Taq DNA polymerase (Life Technologies Japan) with the primer sets listed in Table 1.

Immunostaining ES and TS cells were cultured on gelatin-coated glass coverslips in a six-well plate. Colonies of ES or TS cells were fixed with 4% paraformaldehyde/PBS for 10 min and then permeabilized with 0.1% Triton X-100 for 5 min at room temperature. The fixed samples were incubated in Blocking One solution (Nacalai Tesque, Kyoto, Japan) for 30 min, and then incubated with the primary antibody for 2 h, followed by the secondary antibody for 1 h at room temperature. The following antibodies were used: rabbit immunoglobulin (IgG) anti Oct3/4 (1:400; Santa Cruz Biotech), rabbit IgG anti Cdx2 (1:50; Cell Signaling Technology). DAPI was used for nuclear staining.

Cell proliferation assay Cells were seeded on a gelatin-coated 96-well plate at 5×10^3 cells/well, in the appropriate medium for ES or TS cell culture ± different concentrations of TLR ligands. The proliferative rates of these cells were evaluated 36–60 h after poly(I:C) treatment using a WST-8 cell viability test kit (Nacalai Tesque).

RESULTS

Establishment of a TS cell line Morulae were collected from BALB/cA female mice 2.5 day post-coitum (dpc), and were cultured to blastocysts. Three blastocysts were cultured on the feeder layer in the TS medium. During the culture, the blastocysts hatched and attached to the feeder layer within 2 days. On day 3–4, the blastocyst outgrowths emerged and grew out. The growing outgrowths were trypsinized into single cells, which were sown on the feeder layer again. When TS-like colonies became visible on culture day 7–16, seven independent colonies were picked, and were passaged

to a new feeder layer following trypsinization. Finally, a cell line was established as CAT1. CAT1 was isolated from MEF feeder cells and cultured on a gelatin-coated dish without a feeder layer (Fig. 1A). RT-PCR was used to compare trophectoderm-specific gene expression in CAT1 cells to that in the ES cell line, ST1, maintained without the feeder layer. The ST1 ES cell line was derived from the same mouse strain, BALB/cA, as was CAT1. *Cdx2*, which is a representative trophoblast-specific gene (24) was strongly expressed in CAT1, but not in ST1. *Oct3/4*, which is one of the representative ES- or ICM-specific genes (25,26), was strongly detected in ST1, but not in CAT1 (Fig. 1C). Cdx2 protein was also confirmed in CAT1, but not in ST1, while *Oct3/4* protein was present in ST1, but not in CAT1, as determined by the immunostaining experiments in Fig. 1D–G. As shown in Fig. 1B, CAT1 could be differentiated into trophoblastic giant–like cells without FGF4 and heparin. These results suggest that we succeeded in establishing a TS cell line, CAT1, from BALB/cA blastocysts. The sex of the donor blastocysts that gave rise to ST1 and CAT1 was determined to be male and female, respectively, by genomic PCR examination of the sex-determining region of *Chr* Y (*Sry*) and *Hprt* genes, which are located on the Y- (27) and X-chromosomes (28), respectively (Fig. 1H). Feeder-free CAT1 and ST1 were used to represent blastocyst trophectoderm and ICM, respectively, for the following experiments.

Expression of TLRs in ES and TS cells Both ST1 and CAT1 were cultured on gelatin-coated dishes without the feeder layer because the feeder cells were mitomycin C–treated MEFs, which strongly express some TLRs and other immune molecules. ST1 and CAT1 were cultured to confluent without any stimulation, and then

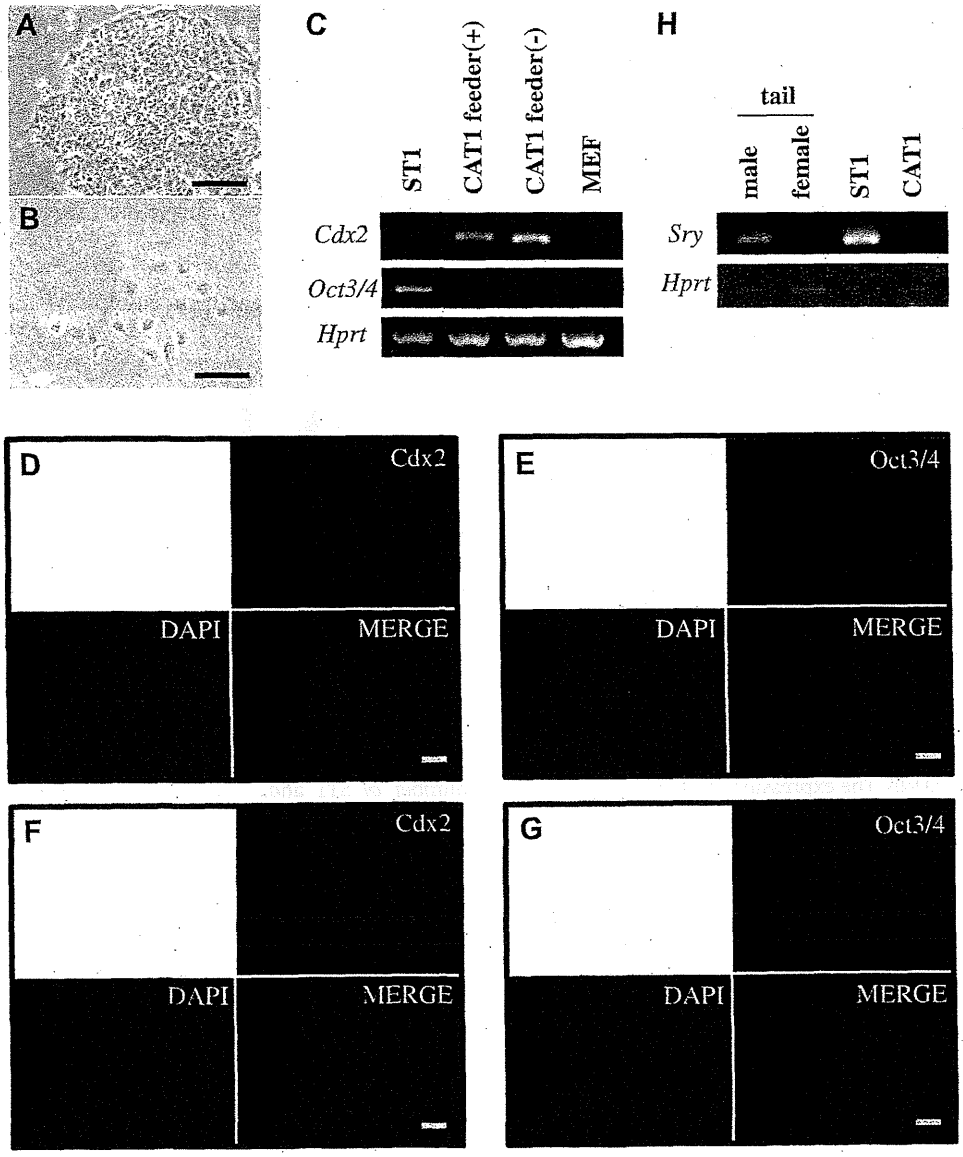

FIG. 1. Characterization of CAT1 as trophoblast stem cells. The CAT1 cell line was isolated from BALB/c mouse blastocysts. (A, B) Differentiation of TS cells into trophoblast giant cells. CAT1 cells were cultured in TS medium with (A) and without (B) growth factors. Scale: 100 μm (C) RT-PCR analysis of CAT1 and ST1, an embryonic stem cell line derived from BALB/c mice. Cdx2: trophoblast-specific gene. Oct3/4: undifferentiated state specific gene. (D–G) Immunostaining of ST1 (D, E) and CAT1 (F, G). (D, F) Cdx2 (red) and DAPI (blue). (E, G) Oct3/4 (red) and DAPI (blue). (H) Determination of the sex of ST1 and CAT1 donor blastocysts via genomic PCR of *Sry* and *Hprt*. (For interpretation of the references to colour in this figure legend, the reader is referred to the web version of this article.)

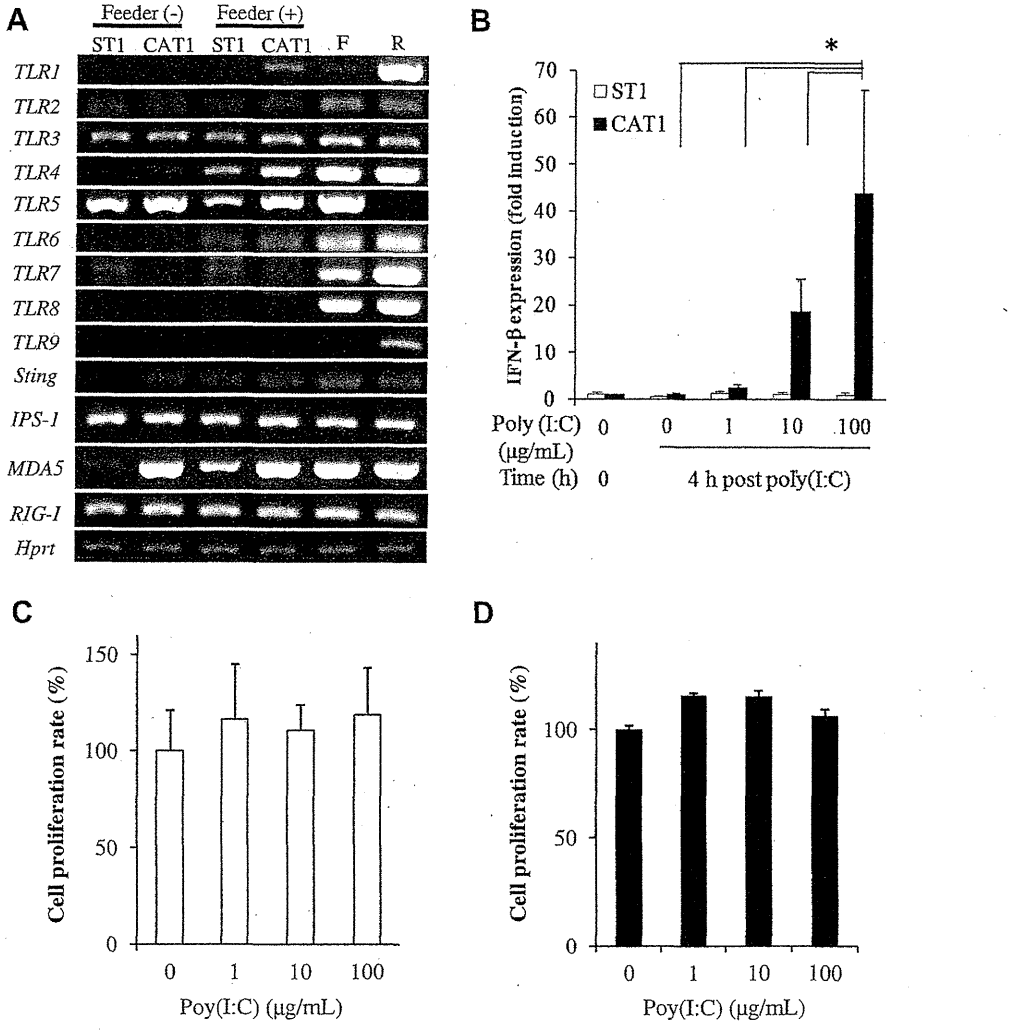

FIG. 2. TLR expression in ST1 and CAT1 cells, and IFN-β expression after poly(I:C) stimulation. (A) TLRs expression in ST1 and CAT1 was examined by RT-PCR. ST1 and CAT1 were cultured both with and without a feeder layer. TLR1-9: 40 cycles, Sting: 25 cycles, RIG-I: 30 cycles, *Hprt*: 22 cycles. F: MEF feeder layer, R: RAW264. Primers are listed in Table 1. (B) ST1 and CAT1 were stimulated by 1, 10, or 100 μg/mL of poly(I:C) for 4 h. IFN-β mRNA expression levels in these cells were measured by real-time PCR. Open bars, ST1; closed bars, CAT1. Data are represented as mean ± S.E. of triplicate measurements. $^*p < 0.01$ (Student's t-test). (C, D) Cell proliferation of ST1 (C) and CAT1 (D) after stimulation by 1, 10, or 100 μg/mL of poly(I:C) was detected 24 h after stimulation using the WST-8 proliferation assay.

the cells were collected for RNA preparation. Total RNA was reverse-transcribed to cDNA. The expression of pattern recognition receptor genes was investigated in ST1 and CAT1 by RT-PCR (Fig. 2A). Expression of TLR2, -3, -5, and -7 was detected in ST1, while expression of TLR2, -3, and -5 was observed in CAT1. Furthermore, RIG-I and Sting, which detect microbial-derived nucleic acids independent of the TLR pathway, were both expressed in ES and TS cells. By contrast, MDA5, another sensor of double stranded RNA, was strongly detected in CAT1 but not in ST1.

IFN-β expression in ES and TS cells after stimulation by dsRNA ST1 and CAT1 cells were stimulated by the addition of 1, 10, or 100 μg/mL polyinosinic:polycytidylic acid [poly(I:C)], which is a TLR-3 ligand. Both ST1 and CAT1 were stimulated by poly(I:C), and then the cells were collected for RNA preparation at 0 and 4 h post-stimulation. Total RNA was reverse-transcribed to cDNA. The amount of *IFN-β* expression was quantified in each sample using real-time PCR. The expression of *IFN-β* was induced in TS cells, but not ST1 cells, after poly(I:C) stimulation at 4 h (Fig. 2B). Cell viability was measured after poly(I:C) stimulation (Fig. 2C and D). The number of ST1 and CAT1 cells in the treated cultures did not change significantly.

IFN-inducible gene activation in ES and TS cells after IFN-β treatment The expression of IFNAR1, a receptor of type-I interferon, was detected in both ST1 and CAT1 cells (Fig. 3A). To determine the responsiveness of ES and TS cells to IFN-β, ST1, and CAT1 were stimulated by 10^4 unit/ml of IFN-β. Then, we examined the expression of PKR and OAS1a, which are representative genes induced by type-I IFN (α/β), and the cell proliferation rate. As shown in Fig. 3D and E, PKR was induced in both ST1 and CAT1, while OAS1a was only induced in ST1. However, cell proliferation was only suppressed in CAT1 (Fig. 3B and C).

Poly(I:C) stimulation of ES/TS co-cultures As shown in Fig. 4, GFP-expressing ST1 ($ST1^{Green}$) and DsRed-expressing CAT1 ($CAT1^{Red}$) were established to distinguish between ES cells and TS cells in culture. Then, the two cell types were co-cultured, and stimulated with 100 μg/mL poly(I:C). The cells were collected for

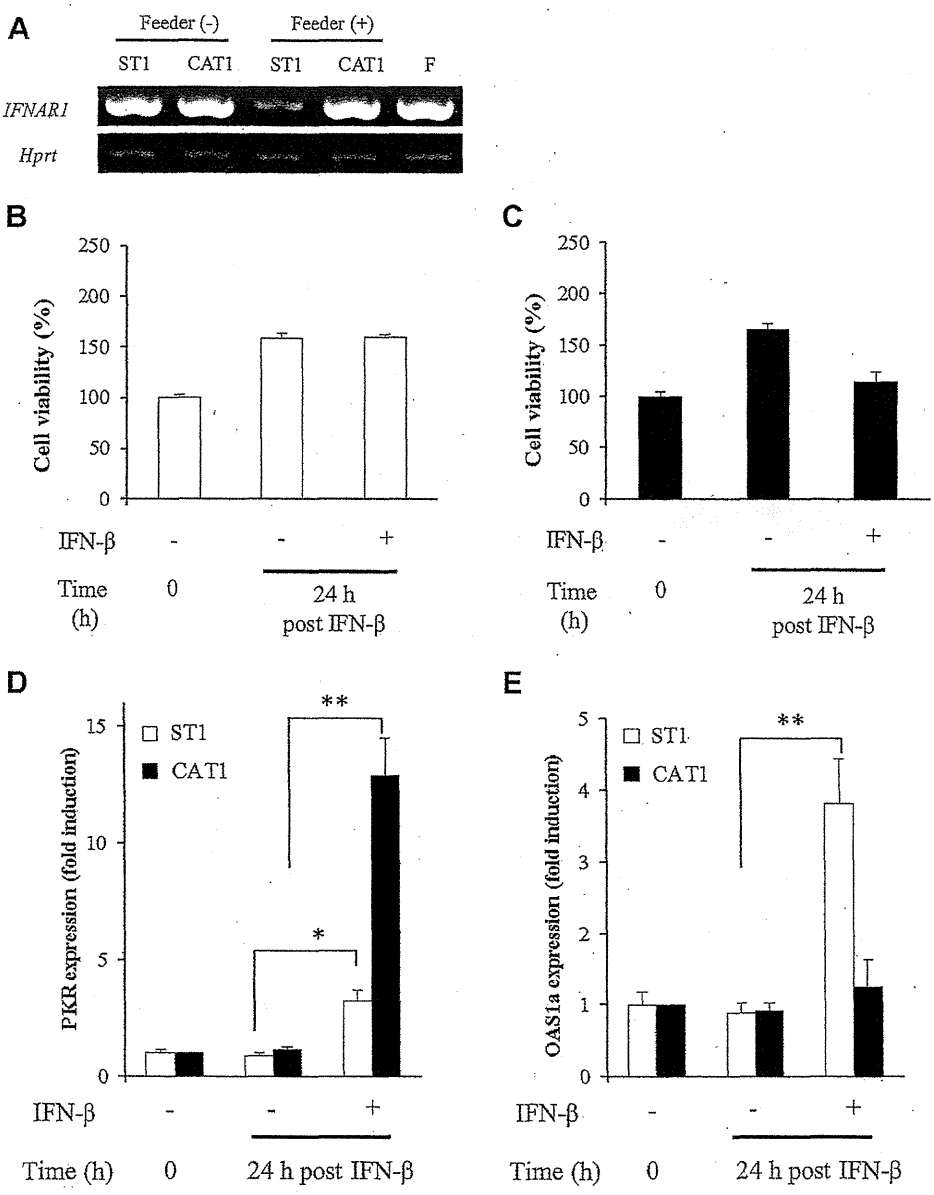

FIG. 3. Interferon-inducible gene expression and cell proliferation after IFN-β treatment. (A) IFNAR1 expression was detected by RT-PCR (25 cycles). F: MEF feeder layer. (B, C) ST1 (B) and CAT1 (C) cell numbers were measured 24 h after the addition of 10^4 unit/ml of IFN-β by using the WST-8 cell proliferation assay; $n = 6$. (D, E) PKR and OAS1a expression was measured by real-time PCR. Open bars, ST1; closed bars, CAT1. Data are represented as mean ± S.E. of triplicate measurements. $^*p < 0.01$; $^{**}p < 0.001$ (Student's *t*-test).

RNA preparation at 0, 4, and 24 h after poly(I:C) stimulation. IFN-β, PKR, and OAS1a expression levels were analyzed using real-time PCR (Fig. 5A–C). Under co-culture conditions, both IFN-β and PKR were induced 4 and 24 h after stimulation. Interestingly, OAS1a was induced at 24 h under co-culture conditions, but was not induced when either cell type was cultured alone and stimulated with poly(I:C).

DISCUSSION

It is hard to collect enough early-stage embryos to perform molecular biology experiments. Because ES and TS cells can proliferate and expand in culture, they represent useful tools for the investigation of cellular communication within blastocysts, and as an *in vitro* model of blastocyst function. Microbes first encounter the trophectoderm layer, which is the outermost layer of the blastocyst. Therefore, it is important to study the immune system in the trophectoderm. However, to date, there are some reports describing the expression of TLRs in ES cells (14–16), but none that deal with TS cells. Furthermore, in those studies, the genetic background of all of the ES cell lines examined was the 129 strain. By contrast, the BALB/c and C57BL/6 genetic strains are popular for studies of the immune system, and therefore, experiments in those lines would be relatively easy to correlate with other immunological studies in mice. Here, we succeeded in establishing a trophoblast stem cell line, CAT1, from the BALB/c mouse strain. The ES cell line, ST1, had already been established from the BALB/c background (17). Therefore, the immune responses in ST1 and CAT1 cell lines could be serve as *in vitro* models of the immune function in the mouse blastocyst ICM and trophectoderm, respectively, in the BALB/c genetic background.

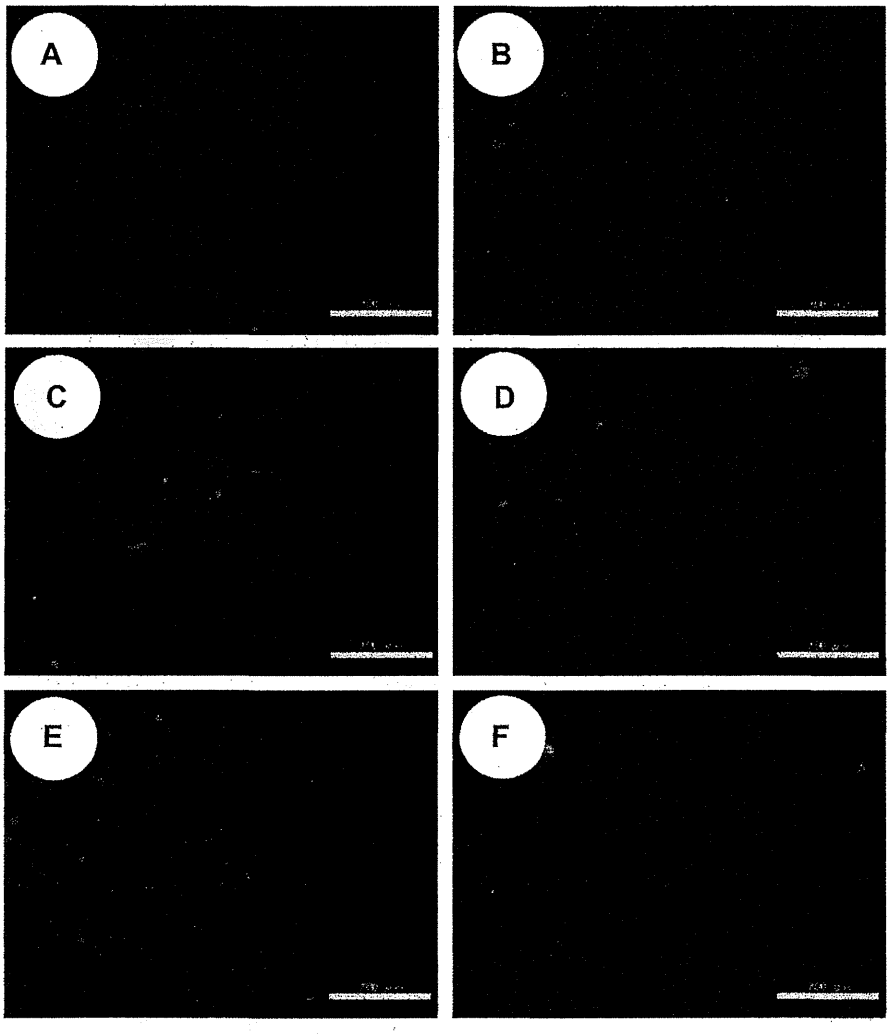

FIG. 4. Co-culture of ST1^{Green} and CAT1^{Red} with poly(I:C). Microscopic images of ST1^{Green} or CAT1^{Red} monocultures and co-cultures treated with 100 μg/mL poly(I:C); scale: 200 μm. (A, B) Monoculture of ST1^{Green}. (C, D) Monoculture of CAT1^{Red}. (E, F) Co-culture of ST1^{Green} and CAT1^{Red}. (A, C, E) non-stimulation. (B, D, F) Cells were stimulated by 100 μg/mL of poly(I:C). (For interpretation of the references to colour in this figure legend, the reader is referred to the web version of this article.)

CAT1 cells strongly expressed TLR2, -3, and -5 and poly(I:C)-induced IFN-β production in these cells. However, IFN-β could not be induced in ST1 cells by poly(I:C) (Fig. 2A and B). IFN-β is produced predominantly by fibroblast cells (9–11), but poly(I:C) can also induce IFN-β in TS cells, suggesting that the blastocyst trophectoderm may have the potential to produce IFN-β in response to a microbial infection. By contrast, ES cells did not produce IFN-β after poly(I:C) stimulation (Fig. 2B), but they did express the type-I IFN receptor (Fig. 3A). Recently, Wang et al. demonstrated that La Crosse virus (LACV) infection induced type-I IFN in mouse fibroblasts but not in mouse ES cells, which had a much lower expression of MDA5 and TLR-3 as compared to fibroblasts (29). We consider that a more physiologically relevant comparison is to assess the relative expression levels of these genes between ES and TS cells, rather than in fibroblasts where IFN-β is highly produced (9–11). TLR-3 expression levels in ES cells were almost same as that in TS cells; however, MDA5 expression levels in the ES cells were much lower than those in the TS cells (Fig. 2A). Therefore, we conclude that IFN-β could not be produced in ES cells due to lower expression of MDA5. IFN-inducible anti-viral proteins, such as PKR and OAS1a, were produced by ES cells after exposure to IFN-β (Fig. 3D and E). Moreover, OAS1a was induced after poly(I:C) stimulation under co-culture conditions (Fig. 5C).

In conclusion, TLR-3 was expressed by both ES and TS cells (Fig. 6A), but appeared to be maximally functional only in TS cells. By contrast, OAS1a was produced only in ES cells. Furthermore, poly(I:C) stimulation of ES-TS co-cultures led to OAS1a expression, presumably through a cooperative feedback loop involving signaling between both cell types. These results suggest that the ICM may have the potential to respond to anti-viral signals by IFN-β by activating downstream anti-viral systems. Taken together, these data suggest that trophectoderm plays the role of a sensor for microbial infection and invasion and produces IFN-β to activate anti-viral systems in both the trophectoderm and the ICM (Fig. 6B).

ACKNOWLEDGMENTS

This study was supported by a Grant-in-Aid for Challenging Exploratory Research (no. 24650254) and for Scientific Research (A) (no. 25242040) from the Japan Society for the Promotion of Science (JSPS) and a Grant-in-Aid for Scientific Research on Innovative Areas (no. 231190003) from the Ministry of Education, Culture, Sports, Science and Technology (MEXT) of Japan. F. Itmainati received a scholarship from Tokyo Institute of Technology Young Scientist Exchange Program (YSEP). We also thank all members of our laboratory for their excellent animal care.

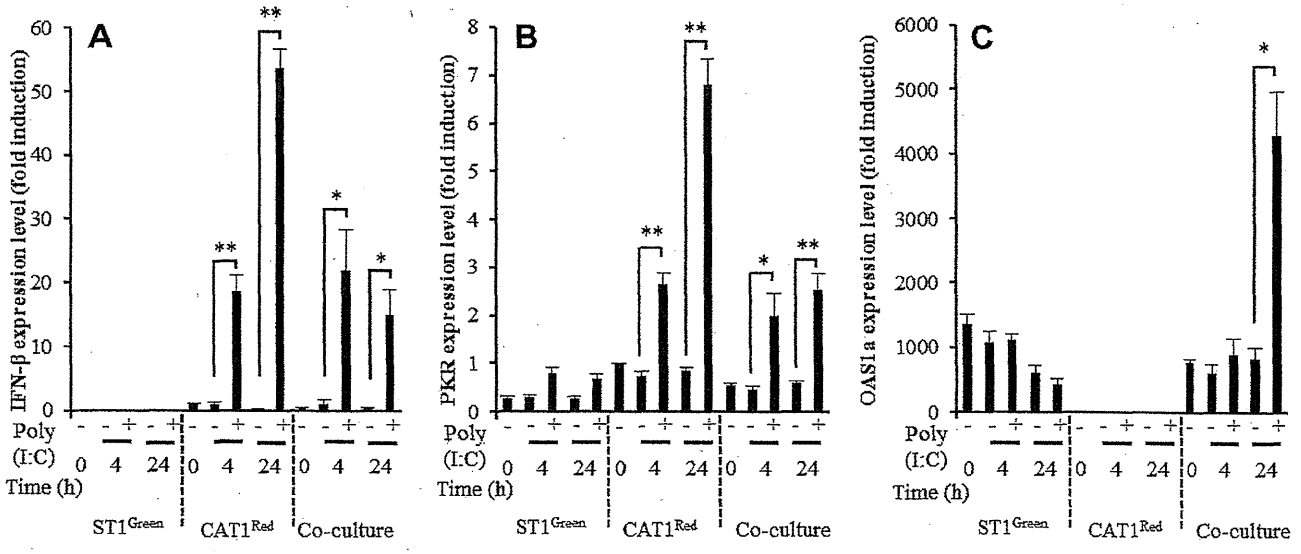

FIG. 5. IFN-β and interferon-inducible gene expression in ST1 and CAT1 co-cultures with poly (I:C). (A) IFN-β, (B) PKR, and (C) OAS mRNA expression in ST1 or CA1 monocultures and co-cultures treated with 100 μg/mL poly(I:C) were measured using real-time PCR. Data are represented as mean ± S.E. of triplicate measurements.*$p < 0.01$; **$p < 0.001$ (Student's *t*-test).

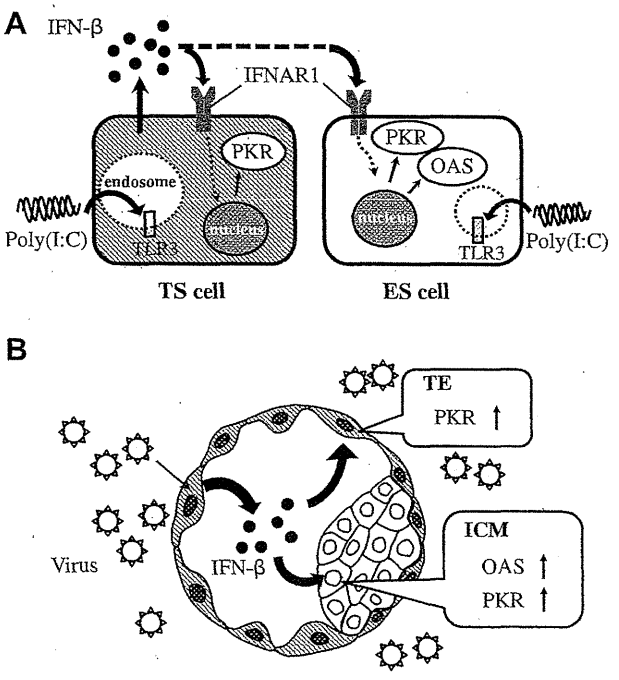

FIG. 6. Our results and hypothesis. (A) Summary of the results. (B) Model describing our hypothesis of how the innate immune system functions in the mouse blastocyst.

References

1. **Kawai, T. and Akira, S.:** The roles of TLRs, RLRs and NLRs in pathogen recognition, Int. Immunol., **21**, 317–337 (2009).
2. **Medvinsky, A. L., Samoylina, N. L., Muller, A. M., and Dzierzak, E. A.:** An early pre-liver intraembryonic source of CFU-S in the developing mouse, Nature, **364**, 64–67 (1993).
3. **Samuel, C. E.:** Antiviral actions of interferons, Clin. Microbiol. Rev., **14**, 778–809 (2001).
4. **Witte, K., Witte, E., Sabat, R., and Wolk, K.:** IL-28A, IL-28B, and IL-29: promising cytokines with type I interferon-like properties, Cytokine Growth Factor Rev., **21**, 237–251 (2010).
5. **Akira, S., Uematsu, S., and Takeuchi, O.:** Pathogen recognition and innate immunity, Cell, **124**, 783–801 (2006).
6. **Hoffmann, J. A.:** The immune response of Drosophila, Nature, **426**, 33–38 (2003).
7. **Lemaitre, B., Nicolas, E., Michaut, L., Reichhart, J. M., and Hoffmann, J. A.:** The dorsoventral regulatory gene cassette spätzle/Toll/cactus controls the potent antifungal response in Drosophila adults, Cell, **86**, 973–983 (1996).
8. **Medzhitov, R., Preston-Hurlburt, P., and Janeway, C. A., Jr.:** A human homologue of the Drosophila Toll protein signals activation of adaptive immunity, Nature, **388**, 394–397 (1997).
9. **Balachandran, S., Thomas, E., and Barber, G. N.:** A FADD-dependent innate immune mechanism in mammalian cells, Nature, **432**, 401–405 (2004).
10. **Ishii, K. J., Kawagoe, T., Koyama, S., Matsui, K., Kumar, H., Kawai, T., Uematsu, S., Takeuchi, O., Takeshita, F., Coban, C., and Akira, S.:** TANK-binding kinase-1 delineates innate and adaptive immune responses to DNA vaccines, Nature, **451**, 725–729 (2008).
11. **Ishikawa, H., Ma, Z., and Barber, G. N.:** STING regulates intracellular DNA-mediated, type I interferon-dependent innate immunity, Nature, **461**, 788–792 (2009).
12. **Dzierzak, E. and Medvinsky, A.:** Mouse embryonic hematopoiesis, Trends Genet., **11**, 359–366 (1995).
13. **Evans, M. J. and Kaufman, M. H.:** Establishment in culture of pluripotential cells from mouse embryos, Nature, **292**, 154–156 (1981).
14. **Zampetaki, A., Xiao, Q., Zeng, L., Hu, Y., and Xu, Q.:** TLR4 expression in mouse embryonic stem cells and in stem cell-derived vascular cells is regulated by epigenetic modifications, Biochem. Biophys. Res. Commun., **347**, 89–99 (2006).
15. **Lee, S. H., Hong, B., Sharabi, A., Huang, X. F., and Chen, S. Y.:** Embryonic stem cells and mammary luminal progenitors directly sense and respond to microbial products, Stem Cells, **27**, 1604–1615 (2009).
16. **Taylor, T., Kim, X. J., Ou, X., Derbigny, W., and Broxmeyer, H. E.:** Toll-like receptor 2 mediates proliferation, survival, NF-κB translocation, and cytokine mRNA expression in LIF-maintained mouse embryonic stem cells, Stem Cells Dev., **19**, 1333–1341 (2010).
17. **Sato, H., Takahashi, M., Ise, H., Yamada, A., Hirose, S., Tagawa, Y., Morimoto, H., Izawa, A., and Ikeda, U.:** Collagen synthesis is required for ascorbic acid-enhanced differentiation of mouse embryonic stem cells into cardiomyocytes, Biochem. Biophys. Res. Commun., **342**, 107–112 (2006).
18. **Ogawa, S., Tagawa, Y., Kamiyoshi, A., Suzuki, A., Nakayama, J., Hashikura, Y., and Miyagawa, S.:** Crucial roles of mesodermal cell lineages in a murine embryonic stem cell-derived in vitro liver organogenesis system, Stem Cells, **23**, 903–913 (2005).
19. **Tanaka, S., Kunath, T., Hadjantonakis, A. K., Nagy, A., and Rossant, J.:** Promotion of trophoblast stem cell proliferation by FGF4, Science, **282**, 2072–2075 (1998).
20. **Niwa, H., Yamamura, K., and Miyazaki, J.:** Efficient selection for high-expression transfectants with a novel eukaryotic vector, Gene, **108**, 193–199 (1991).
21. **Kanegae, Y., Lee, G., Sato, Y., Tanaka, M., Nakai, M., Sakai, T., Sugano, S., and Saito, I.:** Efficient gene activation in mammalian cells by using recombinant adenovirus expressing site-specific Cre recombinase, Nucleic Acids Res., **23**, 3816–3821 (1995).
22. **Ryu, J. Y., Siswanto, A., Harimoto, K., and Tagawa, Y.:** Chimeric analysis of EGFP and DsRed2 transgenic mice demonstrates polyclonal maintenance of pancreatic acini, Transgenic Res., **22**, 549–556 (2013).
23. **Tamai, M., Yamashita, A., and Tagawa, Y.:** Mitochondrial development of the *in vitro* hepatic organogenesis model with simultaneous cardiac mesoderm differentiation from murine induced pluripotent stem cells, J. Biosci. Bioeng., **112**, 495–500 (2011).

24. **Strumpf, D., Mao, C. A., Yamanaka, Y., Ralston, A., Chawengsakwophak, K., Beck, F., and Rossant, J.:** Cdx2 is required for correct cell fate specification and differentiation of trophectoderm in the mouse blastocyst, Development, **132**, 2093–2102 (2005).
25. **Nichols, J., Zevnik, B., Anastassiadis, K., Niwa, H., Klewe-Nebenius, D., Chambers, I., Schöler, H., and Smith, A.:** Formation of pluripotent stem cells in the mammalian embryo depends on the POU transcription factor Oct4, Cell, **95**, 379–391 (1998).
26. **Niwa, H., Miyazaki, J., and Smith, A. G.:** Quantitative expression of Oct-3/4 defines differentiation, dedifferentiation or self-renewal of ES cells, Nat. Genet., **24**, 372–376 (2000).
27. **Sinclair, A. H., Berta, P., Palmer, M. S., Hawkins, J. R., Griffiths, B. L., Smith, M. J., Foster, J. W., Frischauf, A. M., Lovell-Badge, R., and Goodfellow, P. N.:** A gene from the human sex-determining region encodes a protein with homology to a conserved DNA-binding motif, Nature, **346**, 240–244 (1990).
28. **Nabholz, M., Miggiano, V., and Bodmer, W.:** Genetic analysis with human–mouse somatic cell hybrids, Nature, **223**, 358–363 (1969).
29. **Wang, R., Wang, J., Paul, A. M., Acharya, D., Bai, F., Huang, F., and Guo, Y. L.:** Mouse embryonic stem cells are deficient in type I interferon expression in response to viral infections and double-stranded RNA, J. Biol. Chem., **288**, 15926–15936 (2013).

Amino Acids (2013) 45:1343–1351
DOI 10.1007/s00726-013-1594-x

ORIGINAL ARTICLE

In vitro recapitulation of the urea cycle using murine embryonic stem cell-derived in vitro liver model

Miho Tamai · Mami Aoki · Akihito Nishimura · Koji Morishita · Yoh-ichi Tagawa

Received: 19 April 2013 / Accepted: 10 September 2013 / Published online: 1 October 2013

Abstract Ammonia, a toxic metabolite, is converted to urea in hepatocytes via the urea cycle, a process necessary for cell/organismal survival. In liver, hepatocytes, polygonal and multipolar structures, have a few sides which face hepatic sinusoids and adjacent hepatocytes to form intercellular bile canaliculi connecting to the ductules. The critical nature of this three-dimensional environment should be related to the maintenance of hepatocyte function such as urea synthesis. Recently, we established an in vitro liver model derived from murine embryonic stem cells, IVL^{mES}, which included the hepatocyte layer and a surrounding sinusoid vascular-like network. The IVL^{mES} culture, where the hepatocyte is polarized in a similar fashion to its in vivo counterpart, could successfully recapitulate in vivo results. L-Ornithine is an intermediate of the urea cycle, but supplemental L-ornithine does not activate the urea cycle in the apolar primary hepatocyte of monolayer culture. In the IVL^{mES}, supplemental L-ornithine could activate the urea cycle, and also protect against ammonium/alcohol-induced hepatocyte death. While the IVL^{mES} displays architectural and functional properties similar to the liver, primary hepatocyte of monolayer culture fail to model critical functional aspects of liver physiology. We propose that the IVL^{mES} will represent a useful, humane alternative to animal studies for drug toxicity and mechanistic studies of liver injury.

Keywords Embryonic stem cell · Liver · Metabolism · Cell polarity · Urea cycle · Ornithine

Abbreviations

ES	Embryonic stem
IVL^{mES}	Murine embryonic stem cell-derived in vitro liver
OTC	Ornithine transcarbamylase
CPS1	Carbamoyl phosphate synthetase 1
ARG1	Arginase 1
ORNT1	Ornithine/citrulline transporter 1
ALT	Alanine aminotransferase
AST	Aspartate aminotransferase
LDH	Lactate dehydrogenase

Introduction

Ammonia, a primary nitrogenous by-product of protein metabolism, must be immediately removed from the circulation to avoid cell/organismal death. In ureotelic organisms, the ammonia in the mitochondria of hepatocytes is converted to urea via the urea cycle. This pathway was discovered by Krebs and Henseleit (1932). L-Ornithine, as well as L-citrulline and L-arginine, is an intermediate of the urea cycle, and it has been reported that the rate of urea formation from ammonia was greatly accelerated by adding any one of these three α-amino acids using thin slices of liver suspended in a buffered aerobic medium.

Electronic supplementary material The online version of this article (doi:10.1007/s00726-013-1594-x) contains supplementary material, which is available to authorized users.

M. Tamai · Y. Tagawa (✉)
Department of Biomolecular Engineering, Graduate School of Bioscience and Biotechnology, Tokyo Institute of Technology, 4259 B51, Nagatsuta-cho, Midori-ku, Yokohama-shi, Kanagawa 226-8501, Japan
e-mail: ytagawa@bio.titech.ac.jp

M. Aoki · A. Nishimura · K. Morishita
Healthcare Products Development Center, Kyowa Hakko Bio Co., Ltd., 2, Miyukigaoka, Tsukuba-shi, Ibaraki 305-0841, Japan

Each of them stimulated urea synthesis to a far greater extent than any of the other common nitrogenous compounds tested (Lehninger et al. 1993). Recently, L-arginine has been reported to stimulate protein synthesis, and to show cytoprotective effects using in vitro model, supporting the results shown in animal models (Kong et al. 2012; Zeng et al. 2012). On the other hand, L-ornithine has been reported to decrease blood ammonia concentration in human and rats (Demura et al. 2010; Cutinelli et al. 1970; and Vogels et al. 1997); however, there has been no report that supplemental L-ornithine can activate the urea cycle in vitro.

We hypothesized that culture models might be insufficient to monitor the urea cycle because it has been shown that primary hepatocyte cultures lack some hepatic functions (Toyoda et al. 2012). Recently, we described the recapitulation of hepatic organogenesis from murine embryonic stem (ES) cells (Ogawa et al. 2005). This murine ES cell-derived in vitro liver model, termed IVL^{mES}, includes both the hepatocyte layer and the accompanying sinusoid vascular-like network, and displays cytochrome P450 activities (Tsutsui et al. 2006). Here, we demonstrated the hepatoprotective effect of L-ornithine using the in vitro IVL^{mES}, but failed to show effects of L-ornithine using apolar primary hepatocyte of monolayer cultures. We conclude that L-ornithine does indeed mediate protective effects on the liver, and that the IVL^{mES} culture system is poised to replace animal models of liver function.

Materials and methods

Reagents

L-Ornithine hydrochloride (Kyowa Hakko Bio, Tokyo, Japan) and ammonium chloride (Sigma–Aldrich, Tokyo, Japan) were dissolved in PBS (100 mM and 4 M) and sterilized by filtration.

Animals

Eight-week-old male BALB/cA Jcl mice were purchased from CLEA Japan, Inc. (Tokyo, Japan). All animal studies have been approved by the Animal Experimentation Committee of Tokyo Institute of Technology.

Isolation of primary hepatocytes from murine liver

Hepatocytes were prepared from anesthetized BALB/cA mice by an in situ two-step collagenase perfusion method (Seglen 1976), with slight modifications. Briefly, murine liver was pre-perfused in situ with Hank's Buffered Salt Solution (HBSS) containing 0.5 mM EGTA. Next, the liver was perfused with 0.015 % collagenase in HBSS. Then, the liver was removed, and the cells were dispersed in ice-cold HBSS without EGTA. The cells obtained were filtered through a 100 μm pore mesh nylon cell strainer (BD Biosciences, MA) and centrifuged twice for 2 min at $500\times g$ to remove non-parenchymal cells. The remaining cells were centrifuged for 2 min at $500\times g$, and then subjected to a 40 % Percoll density gradient centrifugation for 10 min at $1{,}200\times g$. At this stage, cell viability as measured by trypan blue was >90 %. The isolated hepatocytes were plated at a density of 3.0×10^5 cells per well in 12-well plates. Cells were grown in Williams' E Medium containing 10 % (v/v) heat-inactivated FBS, 100 U/mL penicillin and 100 μg/mL streptomycin at 37 °C in a humidified incubator with 5 % CO_2. The medium was replaced after the first 4 h of incubation, and was replaced daily thereafter.

Establishment of in vitro liver model on EHS gel

Formation of in vitro liver model on EHS gel as previously reported (Toyoda et al. 2012). Briefly, HUVECs (0.4×10^6 cell/well in 6-well plates), a representative type of endothelial cells, were seeded on EHS gel. On EHS gel, HUVECs rapidly elongated and generated a network structure. On this network structure of HUVECs, freshly isolated mouse primary hepatocytes (1.0×10^6 cell/well in 6-well plates) were seeded and cultured. The primary hepatocytes migrated toward the HUVEC network and piled next to one another within 24 h, forming a structure that resembled hepatic tissue. This in vitro liver tissue model on EHS gel, which we term IVL_{EHS}, was used in the following experiments.

Culture and differentiation of murine ES cells

The murine ES cell line, ST1, originally established from the BALB/cA strain, was grown on feeder layers of mitomycin C-treated murine embryonic fibroblasts. Cells were grown in Dulbecco's modified Eagle's medium (DMEM) (Invitrogen, Tokyo, Japan) containing 15 % fetal bovine serum (FBS) (Nichirei Biosciences, Tokyo, Japan), 1 mM sodium pyruvate (Invitrogen), 100 μM nonessential amino acids (Invitrogen), 100 μM 2-mercaptoethanol (Sigma-Aldrich Japan, Tokyo, Japan), and 10^3 U/mL leukemia inhibitory factor (LIF) (Chemicon International, CA).

The IVL^{mES} was differentiated from murine ES cells as previously described (Ogawa et al. 2005). Briefly, murine ST1 ES cells were dissociated with 0.25 % trypsin and resuspended in Iscove's modified Dulbecco's medium (IMDM) (Invitrogen) containing 15 % FBS, 1 mM sodium pyruvate, 100 μM nonessential amino acids, and 100 μM 2-mercaptoethanol without LIF. The suspension was then

formed into a hanging drop at a concentration of 1,000 cells per 50 μL. Cells were cultured in an atmosphere containing 5 % CO_2 at 37 °C for 5 days. Under these conditions, cells formed embryoid bodies (EBs). Fifty EBs were plated in each well of a gelatin-coated 6-well plate; the day of plating was denoted as day 0 (A0). In this study, IVL^{mES} were used at A18.

RNA extraction and reverse transcription-polymerase chain reaction analysis

Total RNA was prepared by the acid guanidinium isothiocyanate-phenol–chloroform-isoamyl alcohol method. Total RNA samples (5 μg) were reverse transcribed using a Superscript II first-strand synthesis system (Invitrogen) with an oligo (dT) primer (Invitrogen). PCR was performed using Ex Taq DNA polymerase (TAKARA BIO, Tokyo, Japan) as previously reported (Tamai et al. 2011) with primer sets as shown in Table 1.

Quantification of urea and ammonia concentrations

Culture medium collected during each measurement period was centrifuged for 5 min at 300×*g* to remove cell debris, and the supernatant was stored at −80 °C until use. Urea was detected in the culture medium using a QuantiChrom™ Urea Assay Kit (BioAssay Systems, CA). Ammonia was detected in the culture medium using the Ammonia Test Wako (Wako, Osaka, Japan). Absorbance of the reactions (490 nm for urea; 630 nm for ammonia) was measured using an iMark™ Microplate Reader (Bio-Rad Laboratories, CA). Standard curves were used to calculate the urea and ammonia concentrations in each sample. Urea production, expressed per albumin positive cell number (1.2×10^6) and per 24 h. Albumin positive cell number of the IVL^{mES} was calculated by Immunohistochemical analysis.

Quantification of released liver enzyme activities

After the indicated time periods, culture medium was collected and centrifuged for 5 min at 300×*g*. Then, alanine aminotransferase (ALT), aspartate aminotransferase (AST), and lactate dehydrogenase (LDH) activities in the supernatant were assessed using SPOTCHEM™ EZ SP-4430 and SPOTCHEM™ II LDH (ARKRAY, Kyoto, Japan).

Cell viability assay

The viability of cells was evaluated using a Cell Counting Kit (Dojindo Laboratories, Kumamoto, Japan) or with WST-8, 2-(2-methoxy-4-nitrophenyl)-3-(4-nitrophenyl)-5-(2,4-disulfophenyl)-2*H* tetrazolium, monosodium salt (Dojindo, Tokyo, Japan). The reduction of WST-8 was measured photometrically using an iMark™ Microplate Reader at 450 nm.

Immunohistochemical analysis

IVL^{mES} were cultured on gelatin-coated glass coverslips in 6-well plates, and then fixed with 4 % paraformaldehyde/PBS for 10 min, and permeabilized with 0.1 % Triton X for 5 min at room temperature (RT). Then, the sample was incubated in Blocking One (Nacalai Tesque, Kyoto, Japan) for 30 min, followed by incubation with the primary and secondary antibodies for 2 and 1 h, respectively, at RT. The antibodies included: goat anti-pecam1 (1:200; Santa Cruz Biotechnology, CA); Alexa Fluor 488 donkey anti-goat IgG (1:2000; Invitrogen); rabbit anti-albumin (1:200; Santa Cruz Biotechnology); and Alexa Fluor 594 donkey anti-rabbit IgG (1:2000; Invitrogen). The specimens were mounted in Prolong Gold fluorescent mounting medium and observed using a fluorescence microscope (Olympus, Tokyo, Japan).

Statistical evaluation

The results are expressed as the mean ± SEM. The Student's *t* test was used for the comparison of data from the two groups. The difference between groups was considered significant when $P < 0.05$.

Table 1 RT-PCR primer sequences

Gene name	Forward (5′–3′)	Reverse (5′–3′)
Carbamoyl phosphate synthetase 1 (Cps1)	TGCCAATGTGACTACGAAGC	AAATTGCAGGGACCTTTTCC
Arginase, liver (Arg1)	TCACCTGAGCTTTGATGTCG	TTACCCTCCCGTTGAGTTCC
Ornithine transcarbamylase (Otc)	GAAAGGGTCACACTTCTGTGG	GAGCAAAGCCTGTTTCTGTGG
Ornithine transporter 1 (Ornt1)	GTGGTCCGTAAAGTGGTTGG	TGAGAGCCCATGGTAGAAGC
Albumin	CAGGATTGCAGACAG	GCTACGGCACAGTGC
Hypoxanthine-guanine phosphoribosyltransferase (hprt)	AGCTTTACTAGGCAGATGGC	GTAATGATCAGTCAACGGGG

Results

L-Ornithine enhances urea production in in vitro liver tissue model, but not in cultured primary hepatocytes

Released hepatic enzymes, such as ALT, AST, and LDH, were measured in primary hepatocyte medium 24 h after the addition of NH_4^+ at a variety of doses. The activity levels of the three enzymes increased in a dose-dependent manner in response to NH_4^+ (Fig. 1a). By contrast, cell viability, as determined by WST-8 activity levels, decreased in a NH_4^+ dose-dependent manner (Fig. 1b). Urea production in the cultures increased with the addition of NH_4^+ up to 10 mM, but decreased at NH_4^+ concentrations exceeding 20 mM NH_4^+, i.e., NH_4^+-induced cell death at high concentrations (Fig. 1c). Therefore, to test the protective effects of L-ornithine, we used NH_4^+ concentrations of 20 mM or more in the subsequent experiments.

If NH_4^+ could activate the urea cycle in cultured primary hepatocytes, we would expect to see suppression of ammonia-induced cell death in the cultures. L-Ornithine was added to the medium of the primary hepatocytes or HUVEC co-cultured on type I collagen or EHS gel-coated plastic dishes and IVL_{EHS}. In the case of monolayer culture on type I collagen, no increase in urea production was observed in the culture medium (Fig. 1d). In contrast, the increase in urea levels was detected in the IVL_{EHS} (Fig. 1e), but the signal was not robust enough for the method to be used as a model system for this study.

An in vitro liver model derived from murine ES cells, IVL^{mES}, was prepared from the embryonic stem cell line, ST1, which was originally established from BALB/cA

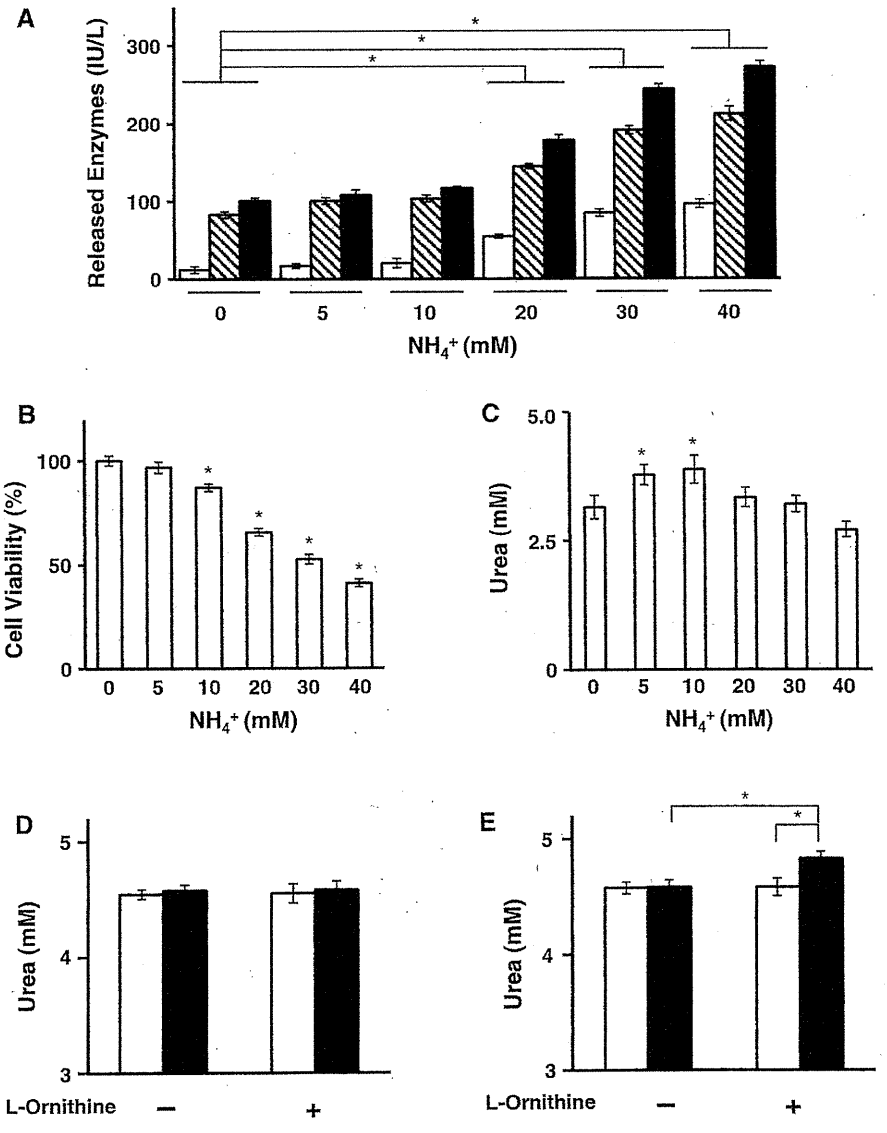

Fig. 1 Ammonia sensitivity of primary hepatocyte cultures. **a** Activity levels of released liver enzymes: alanine aminotransferase (ALT, *white bars*); aspartate aminotransferase (AST, *hatched bars*); and lactate dehydrogenase (LDH, *black bars*). **b** Cell viability, as assessed by the WST-8 assay, of primary hepatocyte cultures 24 h after the addition of 0–40 mM NH_4^+. **c** Urea concentrations in the medium of primary hepatocyte cultures 24 h after the addition of 0–40 mM NH_4^+. **d, e** Urea production in the medium of primary hepatocytes, cultured on type I collagen-and EHS gel-coated plastic dishes or IVL_{EHS} and IVL^{mES}, 24 h after the addition of 0–100 μM L-ornithine. All data are expressed as the mean ± SE; $^*P < 0.05$

mice. We previously demonstrated that the IVL^{mES} hepatocytes become polarized and express functional transporter proteins (Ogawa et al. 2005; Tsutsui et al. 2006). L-Ornithine was added to the IVL^{mES} culture medium, and the concentrations of urea in the medium were measured after 24 h. Urea production increased with respect to the amount of L-ornithine added to the culture (Fig. 2a).

L-Ornithine protects against ammonium-induced hepatocyte death in the IVL^{mES}

To assess whether L-ornithine was protective against NH_4^+-induced hepatocyte death in the IVL^{mES}, L-ornithine was added to the culture medium in the presence of NH_4^+. The expression of urea cycle-related genes was observed in the IVL^{mES} cells, even after addition of NH_4^+ (Fig. 2b). NH_4^+ decreased cell viability in a dose-dependent fashion in the absence, but not the presence, of L-ornithine (Fig. 2c). In particular, at doses of 30–40 mM NH_4^+, cell viability levels were significantly higher in the presence of L-ornithine as compared to its absence. Because NH_4^+ conversion to urea was enhanced by the addition of L-ornithine in the IVL^{mES} (Fig. 2d), hepatocytes in this culture were protected against NH_4^+-induced cell death.

The protective effect of L-ornithine against ethanol-induced hepatocyte death is observed in the IVL^{mES}, but not in primary hepatocyte cultures

Released hepatic enzymes were measured in the medium of primary hepatocytes 24 h after the addition of ethanol (Fig. 3). The levels of the released hepatic enzymes increased in a dose-dependent manner with increasing levels of ethanol (Fig. 3a), suggesting that ethanol had a dose-dependent effect on cell death. Accordingly, we observed a decrease in cell viability after the same treatments (Fig. 3b). Concentrations of urea and NH_4^+ were measured in the medium of primary hepatocyte cultures 24 h after the addition of ethanol. Treatment with the alcohol decreased urea production (Fig. 3c) and increased the release of NH_4^+ (Fig. 3d) from the hepatocytes. These results indicated that culturing cells in a minimum of 3 % ethanol-induced hepatocyte death; therefore, 3 % ethanol was used in the subsequent experiments.

Next, because L-ornithine could suppress NH_4^+-induced hepatocyte death in the IVL^{mES}, we tested its effects on ethanol-induced hepatocyte death in the same model. Ethanol was added at 3 % to the IVL^{mES} culture medium to induce hepatocyte death. Accordingly, cell viability was decreased, but could be rescued by addition of L-ornithine

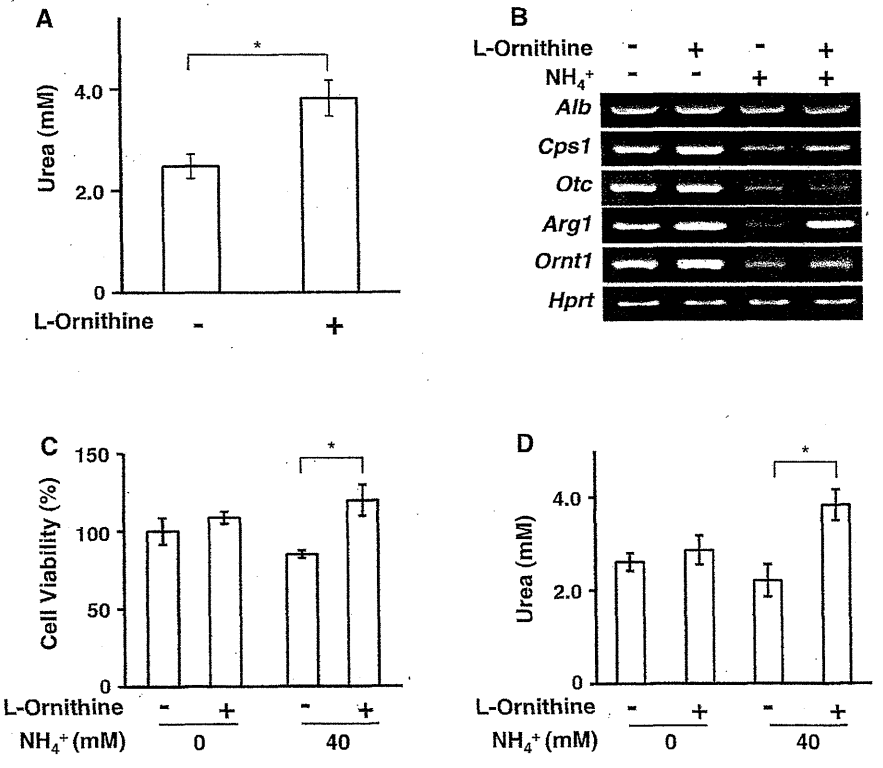

Fig. 2 Protective effects of L-ornithine against NH_4^+-induced cytotoxicity in the murine ES cell-derived liver tissue model, IVL^{mES}. **a** Urea production in IVL^{mES} culture medium 24 h after the addition of 0–100 μM L-ornithine. **b** Expression of albumin and urea cycle-related genes by IVL^{mES} cells 24 h after the addition of 0–100 μM L-ornithine ±40 mM NH_4^+. **c** Cell viability was measured 24 h after the addition of 0–40 mM NH_4^+ ± 100 μM L-ornithine. **d** Urea production in IVL^{mES} culture medium 24 h after the addition of 0 or 100 μM L-ornithine. Data are expressed as the mean ± SE; $^*P < 0.05$

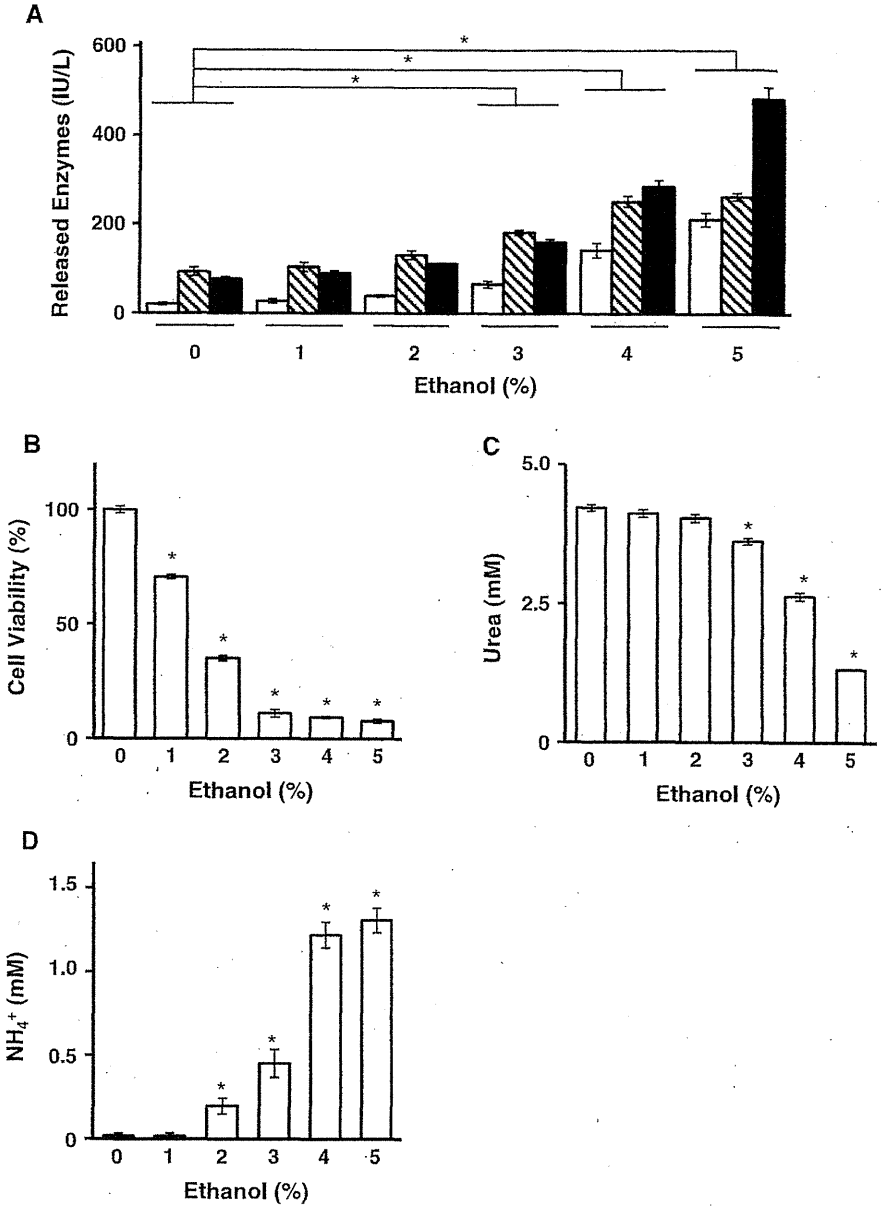

Fig. 3 Ethanol sensitivity of primary hepatocyte cultures. **a** Activity levels of released liver enzymes: alanine aminotransferase (ALT, *white bars*); aspartate aminotransferase (AST, *hatched bars*); and lactate dehydrogenase (LDH, *black bars*). **b** Cell viability, **c** urea production, and **d** ammonia degradation in primary hepatocyte culture medium 24 h after the addition of ethanol. Data are expressed as the mean ± SE; $*P < 0.05$

(Fig. 4a). Concentrations of urea and NH_4^+ in the culture medium were increased and decreased, respectively (Fig. 4b, c), indicating that L-ornithine was protective against ethanol-induced cell death in the IVL^{mES}. Finally, the expression of urea cycle-related genes was also detected in IVL^{mES} cells exposed to ethanol alone or ethanol and L-ornithine (Fig. 4d).

Discussion

It is characteristic that a hepatocyte simultaneously plays a variety of roles in the liver, although other cells generally play a unique role. Cultures of murine primary hepatocytes, obtained by dissociation of the liver into isolated cells, have been used for more than 30 years (Rodriguez-Antona et al. 2000; Tirona et al. 2003), however, it is quite difficult to keep these functions in the in vitro culture. Although many in vitro assays using primary hepatocytes have been reported, when cultured alone, these cells are an imperfect model system to study liver functions in vitro, i.e., experimental results often vary from those obtained by in vivo animal experiments. One reason for this may be that primary hepatocytes cannot proliferate and retain cell type-specific functions when maintained as a monoculture in vitro (Braiterman and Hubbard 2010; Guguen-Guillouzo and Guillouzo 2010; Underhill et al. 2010). In this study, primary hepatocytes were prepared from male BALB/cA

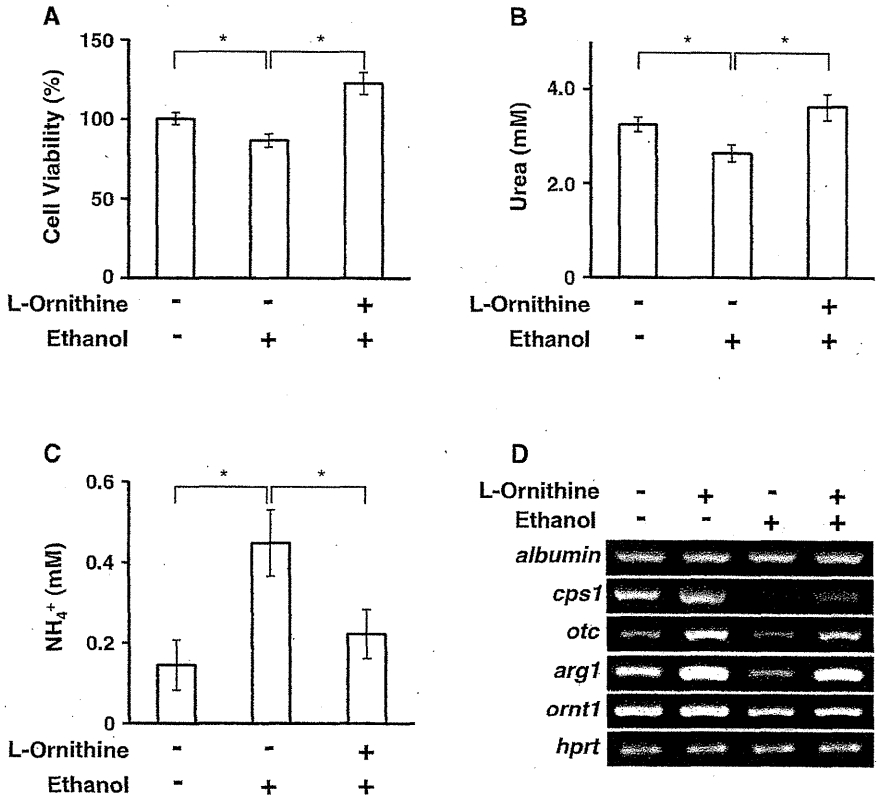

Fig. 4 Protective effects of L-ornithine against ethanol toxicity in the IVL^{mES} system. **a** Cell viability, **b** urea production, and **c** ammonium degradation in IVL^{mES} cells. Data are expressed as the mean ± SE; $*P < 0.05$. **d** Expression of albumin and urea cycle-related genes in IVL^{mES} cells 24 h after the addition of 0–100 μm L-ornithine and 0–3 % ethanol

mice, and cultured on type I collagen-coated plastic dishes. Urea production levels dramatically decreased day-by-day without any stimulation (Supplementary Fig. S1a). To investigate the cause of this reduction, the expression of urea cycle-related genes, such as *carbamoyl phosphate synthetase 1* (*cps1*), *ornithine transcarbamoylase* (*otc*), *arginase 1*(*arg1*), and *ornithine/citrulline transporter 1* (*ornt1*), was assessed by RT-PCR at 0, 1, 4, and 7 days of culture (Supplementary Fig. S1b). The expression of urea cycle-related genes decreased over time, and finally dropped below the limit of detection of the assay, corresponding to the observed decrease in urea production. These results suggested that cultured primary hepatocytes should be used within 1 day of preparation, a directive that we followed for all subsequent experiments in this study.

The liver is composed of parenchymal hepatocytes arranged in cords, and non-parenchymal cells, including sinusoidal endothelial cells forming sinusoidal tubes, and the immune cell population known as Kupffer cells. In particular, sinusoidal endothelial cells are important for the architecture of the liver. Polygonal and multipolar hepatocytes in the liver are surrounded by sinusoids (on their basal side), by the bile canaliculus (at their apical face), and by adjacent hepatocytes (Braiterman and Hubbard 2010). It is only in the context of this tissue architecture that hepatocytes can express their specific functions. Hepatocyte polarity also determines the location of hepatocyte organelles, such as the endoplasmic reticulum and Golgi (Braiterman and Hubbard 2010). For example, the Golgi is positioned between the nucleus and the apical surface. Specific transporters are also preferentially located at specific sides of the hepatocyte. Therefore, hepatocyte polarity exerts a major influence on the cell's physiology. Because primary hepatocytes cultured as a monolayer lose structural polarity, it is difficult to use the culture for assays of hepatic functions, e.g., drug metabolism. Therefore, we aimed to construct a sophisticated culture condition that mimics the situation in the liver, and examine its utility. In our previous reports, we showed that culture of hepatocytes in a model that resembles the structure of hepatic tissue is superior to monolayer culture of primary hepatocytes, both in regard to the maintenance of some hepatic genes and the response to xenobiotics (Toyoda et al. 2012). These findings suggest that this system could be applied to the evaluation of compound.

In the urea cycle, L-ornithine is transported from the cytosol into the mitochondrial matrix via a specific transport system, mitochondrial ORNT1 (Indiveri et al. 1992), and then is carbamylated to citrulline by OTC, which then is exported to the cytosol by ORNT1. Therefore, ORNT1 functions are crucial for hepatocytes to execute the urea cycle. However, in primary hepatocyte cultures, the